Supporting information

A covalent deprotection strategy for assembling supramolecular coordination polymers from metal-organic cages

Matthew L. Schneider,[a] Oliver M. Linder-Patton[a] and Witold M. Bloch*[a]

[a]Department of Chemistry, The University of Adelaide, Adelaide, Australia.

Contents

1. Experimental Section

1.1. Materials and measurements

Unless otherwise stated, all chemicals were obtained from commercial sources and used as received. Compound **4** was synthesised following a standard literature procedure.[1] Triethyl amine (TEA) was distilled from KOH and stored under argon. Tetrahydrofuran (THF) was freshly distilled using a sodium/benzophenone solvent still. Electrospray ionization (ESI) mass spectra were recorded on an Agilent 6230 TOF LCMS. Elemental analyses were performed by the microanalysis laboratory at Macquarie University. Infrared spectra were collected on a Perkin-Elmer Spectrum 100 using a UATR sampling accessory. Thermal gravimetric analysis (TGA) was performed on a Perkin-Elmer STA-6000 instrument or on a TA Instruments Discovery TGA under a constant flow of N_2 at a temperature increase rate of 10 °C/min

High field NMR spectra were recorded using an Agilent 500 MHz or 600 MHz spectrometer. Whilst the anomalous paramagnetism of the Cu_2 paddle-wheel precluded a complete assignment of proton resonances of $\mathbf{C^{Boc}}$ and $\mathbf{C^{Fmoc}}$, resonances not immediately adjacent to the metal nodes were clearly resolved and could be assigned (Fig S5 and S6).[2,3]

Powder X-ray diffraction data were collected on a Bruker Advanced D8 diffractometer (capillary stage) using Cu Kα radiation (λ = 1.5418 Å, 50 kW/40mA) Simulated powder X-ray diffraction patterns were generated from the single crystal data using Mercury 4.3.1

Gas sorption isotherm measurements were performed on a Micromeritics 3Flex Surface Characterisation Analyser. UHP grade (99.999 %) N_2 was used for all measurements. Temperatures were maintained at 77 K using a cryo-cooler. The isotherms were then analysed to determine the Brunauer Emmet-Teller (BET) surface area and pore-size distribution using the MicroActive software (Version 3.00, Micromeritics Instrument Corp. 2013).

Gas mixtures arising from solid-state $\mathbf{C^{Boc}}$ deprotection were analysed by an RGA (Stanford Research Systems, RGA200) which is housed in a vacuum chamber with an electron multiplier, controlled via Stanford Research Systems RGA software for data collection. Pressure is measured by a Bayard-Alpert ionisation gauge with a tungsten filament (Duniway, T-CFF-275) monitored via a combined ion and thermocouple controller (Agilent Technologies, XGS-600). The system is pumped via an oil-free turbo-pump (Agilent TwisTorr 84FS) backed by a rotary vane pump (Edwards, E2M8) with an oil trap (Duniway IFT-NW25-4). The m/z 41 peak used to quantify the production of iso-butylene was calibrated using a CO_2/iso-butylene mixture of 1.68 bar 1-butene and 1.94 bar CO_2 with a total pressure of 3.63 bar in the reaction cell.

1.2. Synthesis of ligands L^{1-3}

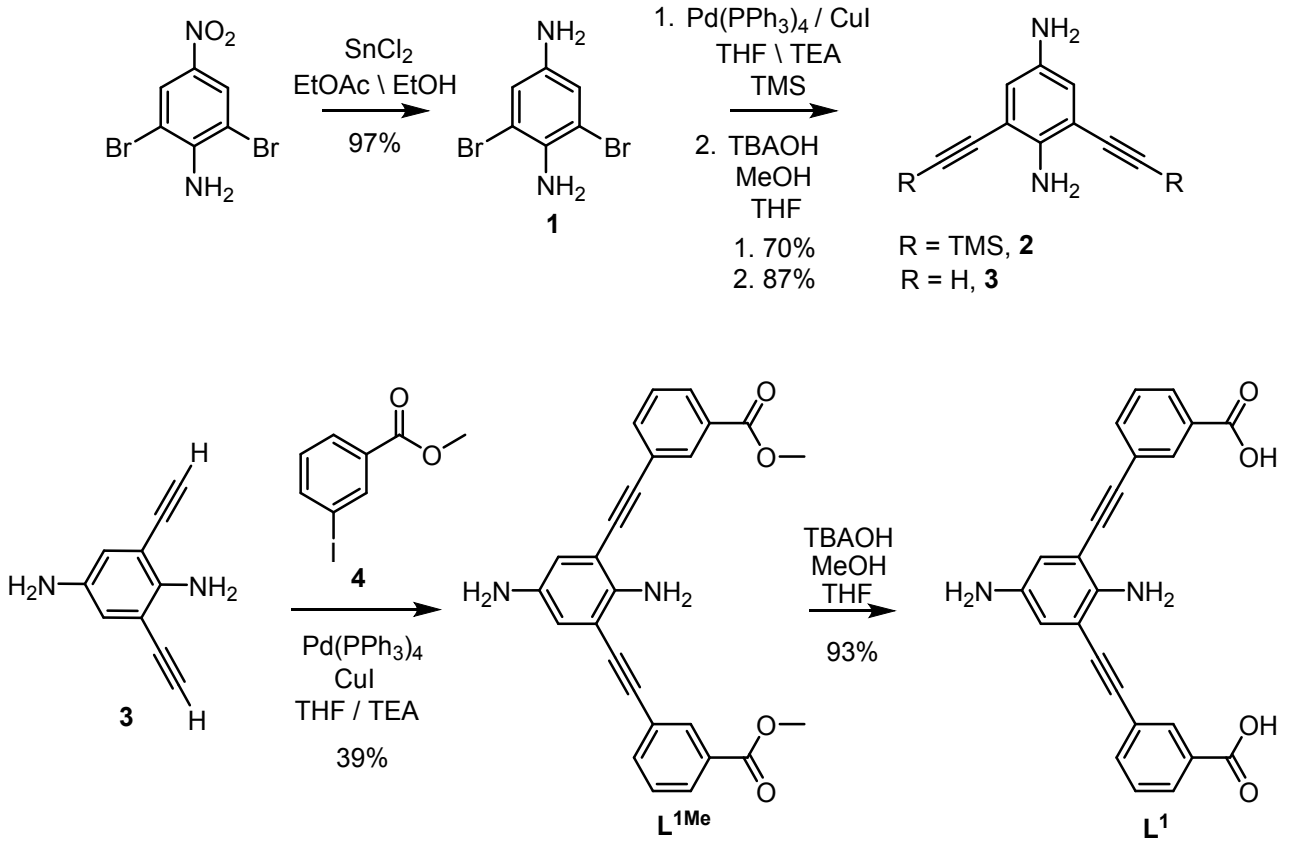

Scheme 1

*1.2.1. 2,6-dbromo-4-nitrophenol (**1**)*

Tin (II) chloride (21.9 g, 97 mmol) was combined with 2,6-dibromo-4-nitroanaline (5.00 g, 17.8 mmol) in 1:1 THF/EtOH (74 mL). The reaction mixture was stirred at 50 °C for 16 h under a nitrogen atmosphere. The solvent was removed under reduced pressure and NaOH (2 M, 250 mL) was added to the residue. After this, the reaction mixture was stirred at 25 °C for a further 2.5 h. The resulting aqueous mixture was extracted with diethyl ether (4 x 40 mL), and the combined organic layers were washed once with brine (50 mL) and then dried over $MgSO_4$. The solvent was removed under reduced pressure to afford 2,6-dibromobenzene-1,4-diamine **1** as white crystals (4.62 g , 97%); ^{1}H NMR (500 MHz, $CDCl_3$) δ 6.83 (s, 2H), 4.08 (s, 2H), 3.41 (s, 2H); ^{13}C NMR (125 MHz, $CDCl_3$) δ 141.85, 137.23, 121.85, 112.55; ESI-MS: calculated for $C_6H_6Br_2N_2$ $[M+H]^+$ 266.8911, found 266.8950.

*1.2.2. 2,6-diethynylbenzene-1,4-diamine (**3**)*

In a Schlenk vessel, **1** (0.20 g, 0.75 mmol) was dissolved in THF (3 mL) and TEA (2.5 mL) under an argon atmosphere. Once the solvent was degassed with argon, $Pd(PPh_3)_4$ (0.010 g, 0.0086 mmol) and CuI (0.0017 g, 0.0089 mmol) were added to the solution. After the addition of ethynyltrimethylsilane (0.14 mL, 0.99 mmol), the reaction vessel was sealed and the mixture was heated at 80 °C for 16 h. Upon completion, the reaction mixture was diluted with EtOAc (15 mL), filtered, and concentrated under reduced pressure. The crude residue was purified via column chromatography (hexane : EtOAc = 6:1) to afford 2,6-bis((trimethylsilyl)ethynyl)benzene-1,4-diamine **2** as a brown solid (0.160 g, 70%); ^{1}H NMR (500 MHz, $CDCl_3$) δ 6.71 (s, 2H), 4.43 (s, 2H), 0.24 (s, 18H). To a solution of **2** (1.70 g, 5.65 mmol) in 1:1 MeOH/DCM (20 mL), K_2CO_3 (1.76 g, 12.77 mmol) was added and the suspension was stirred at 25 °C for 2 h. After this period, water (20 mL) was added, and the mixture was extracted with DCM (3 x 20 mL). The combined organic extracts were dried over $MgSO_4$ and concentrated under reduced pressure to afford 2,6-diethynylbenzene-1,4-

diamine **3** as a brown solid (0.81 g, 87%); V_{max} (neat, cm^{-1}): 3396 (w, N-H), 3325 (w), 3269 (w, C-H), 3218 (w), 2094 (s. C=C), 1591 (m, C=C), 691 (s, N-H), 659 (s, N-H); ^1H NMR (500 MHz, $CDCl_3$) δ 6.75 (s, 2H), 4.44 (s, 2H), 3.36 (s, 2H), 3.29 (s, 2H); ^{13}C NMR (125 MHz, $CDCl_3$) δ 144.30, 137.15, 121.23, 107.80 , 83.00, 80.56; ESI-MS: calculated for $C_{10}H_8N_2$ $[M+H]^+$ 157.0766, found 157.0750

1.2.3. L^{1Me}

2,6-Diethynylbenzene-1,4-diamine **3** (0.80 g, 2.6 mmol) was combined with methyl 3-iodobenzoate **4** (2.95 g, 11.25 mmol) in 1:1 THF/TEA (40 mL) in a Schlenk vessel under argon. Once the solvent was degassed with argon, $Pd(PPh_3)_4$ (0.155g, 0.13 mmol) and CuI (0.026g, 0.13 mmol) were added to the mixture. The reaction vessel was sealed and the reaction mixture was heated at 85 ° C for 18 h. The reaction mixture was diluted with EtOAc (25 mL), filtered, and the solvent was removed under reduced pressure. The crude residue was purified via column chromatography (hexane : EtOAc = 1:1) to afford dimethyl 3,3'-((2,5-diamino-1,3-phenylene)bis(ethyne-2,1-diyl))dibenzoate (**L^{1Me}**) as a dark yellow solid (0.850 g, 39%); V_{max} (neat, cm^{-1}): 3420 (w, N-H), 3345 (w), 2912 (C-H), 1710 (s, C=O), 1595 (m, C=C), 1452 (m), 1435 (m); ^1H NMR (500 MHz, DMSO) δ 8.16 (t, J = 1.5 Hz, 2H, H_d), 7.97 – 7.95 (m, 2H, H_g), 7.88 – 7.86 (m, 2H, H_e), 7.59 (t, J = 7.8 Hz, 2H, H_f), 6.74 (s, 2H, H_b), 5.08 (s, 2H, H_c), 4.58 (s, 2H, H_a), 3.89 (s, 6H, H_h); ^{13}C NMR (125 MHz, $CDCl_3$) δ 166.51, 142.90, 137.31, 135.69, 132.74, 130.70, 129.44, 128.72, 123.70, 120.41, 108.47, 93.94, 86.69, 52.45; ESI-MS: calculated for $C_{26}H_{20}N_2O_4$ $[M+H]^+$ 425.1501, found 425.1487.

1.2.4. L^1

To a solution of **L^{1Me}** (0.10 g, 0.23 mmol) in dry THF (3 mL), tetrabutylammonium hydroxide (1 M in methanol, 0.76 mL, 0.73 mmol) was added and the mixture was stirred at 50 °C for 3 h. The solvent was removed under an N_2 stream and water (3 mL) was added. The mixture was acidified to pH = 2 with HCl (2 M). The resulting precipitate was isolated under reduced pressure and washed extensively with water. The isolated precipitate was dried for 16 h under vacuum to give 3,3'-((2,5-diamino-1,3-phenylene)bis(ethyne-2,1-diyl))dibenzoic acid (**L^3**) as a dark green solid (0.085 g, 93%); V_{max} (neat, cm^{-1}): 3416 (w, N-H), 3341 (w), 2924 (C-H), 1706 (s, C=O), 1599 (m, C=C), 1435 (m); ^1H NMR (500 MHz, CD_3OD) δ 8.18 (s, 2H, H_d), 8.01 (d, J = 7.7 Hz, 2H, H_g), 7.77 (d, J = 7.7 Hz, 2H, H_e), 7.51 (t, J = 7.8 Hz, 2H, H_f), 6.94 (s, 2H, H_b); ^{13}C NMR (125 MHz, DMSO) δ 166.57, 149.08, 135.59, 132.23, 131.26, 129.46, 129.02, 127.04, 122.63, 106.37, 94.49, 85.68; ESI-MS: calculated for $C_{24}H_{16}N_2O_4$ $[M-H]^-$ 395.1032, found 395.1037.

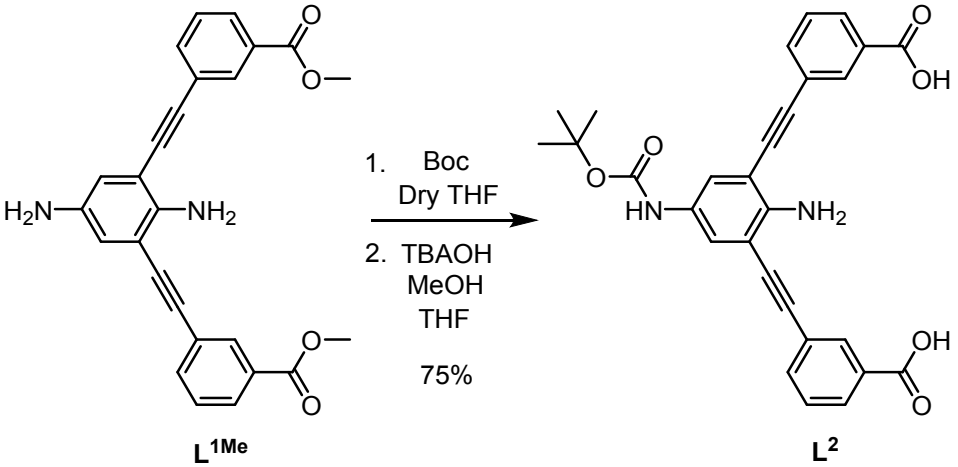

L^{1Me} **L^2**

Scheme 2

1.2.5. L^{2Me}

To a stirred solution of **L^{1Me}** (0.028 g, 0.047 mmol) in dry THF (1.5 mL) di-tert-butyl dicarbonate (28 mg, 0.13 mmol) was added in one portion. The reaction mixture was stirred at 25 °C under N_2 for 5 h. Water (5 mL) was added and the reaction mixture was extracted with DCM (3 x 5 mL). The organic layers were combined and washed once with brine (10 mL) and then dried over $MgSO_4$. The solvent was removed under an N_2 stream to afford dimethyl 3,3'-((2-amino-5-((tert-butoxycarbonyl)amino)-1,3-phenylene)bis(ethyne-2,1-diyl))dibenzoate (**L^{2Me}**) as a crystalline solid (0.020 g, 83%); V_{max} (neat, cm^{-1}): 3361 (w, N-H), 2984 (w, C-H), 2936 (w), 1805 (s), 1764 (s), 1704 (s), 1591 (m), 1540 (m), 1480 (w), 1458 (w), 1438 (w); ^{1}H NMR (500 MHz, $CDCl_3$) δ 8.19 (t, *J* = 1.4 Hz, 2H, H_e), 8.03 – 8.00 (m, 2H, H_h), 7.71 – 7.68 (m, 2H, H_f), 7.45 (t, *J* = 7.8 Hz, 2H, H_g), 7.42 (s, 2H, H_c), 6.26 (s, 1H, H_b), 4.77 (s, 2H, H_d), 3.95 (s, 6H, H_i), 1.56 (s, 9H, H_a); ^{13}C NMR (125 MHz, $CDCl_3$) δ 166.49, 146.89, 135.70, 132.76, 130.71, 129.54, 128.75, 128.67, 123.56, 107.80, 94.30, 86.24, 85.31, 52.46, 28.52, 27.46. ESI-MS: calculated for $C_{29}H_{24}N_2O_6$ $[M-H]^-$ 495.1556, found 495.1555.

1.2.6. L^2

To a solution of **L^{2Me}** (0.220 g, 0.41 mmol) in dry THF (6 mL), tetrabutylammonium hydroxide (1 M in methanol, 1.56 mL, 1.606 mmol) was added and the mixture was stirred at 50 °C for 5 h. After the solvent was removed under an N_2 stream, H_2O (6 mL) was added and the mixture was acidified to pH = 2 with HCl (2 M). The resulting precipitate was isolated under reduced pressure, washed extensively with water and dried under vacuum for 16 h. DMSO (5 mL) and HCl (2 M, 3 mL) were added and the mixture was stirred at rt for 15 minutes. Water (10 mL) was added in one portion and the resulting precipitate was isolated under reduced pressure. Drying the solid under vacuum for 16 h gave 3,3'-((2-amino-5-((tert-butoxycarbonyl)amino)-1,3-phenylene)bis(ethyne-2,1-diyl))dibenzoic acid (**L^2**) as a dark green solid (0.185 g, 91%); V_{max} (neat, cm^{-1}): 3428 (w, N-H), 3345 (w), 2948 (w, C-H), 1708 (s, C=O), 1593 (m, C=C), 1433 (m); ^{1}H NMR (500 MHz, DMSO) δ 13.23 (s, 2H, H_i), 9.13 (s, 1H, H_b), 8.18 (s, 2H, H_e), 7.95 (d, *J* = 6.6 Hz, 2H, H_f), 7.86 (d, *J* = 6.6 Hz, 2H, H_f), 7.56 (t, *J* = 7.8 Hz, 2H, H_g), 7.46 (s, 2H, H_c), 5.59 (s, 2H, H_d), 1.47 (s, 9H, H_a); ^{13}C NMR (125 MHz, DMSO) δ 166.60, 152.98, 145.89, 135.44, 132.06, 131.25, 129.19, 129.02, 128.67, 122.93, 106.00, 93.39, 86.79, 40.43, 28.15; ESI-MS: calculated for $C_{29}H_{24}N_2O_6$ $[M-H]^-$ 495.1556, found 495.1555.

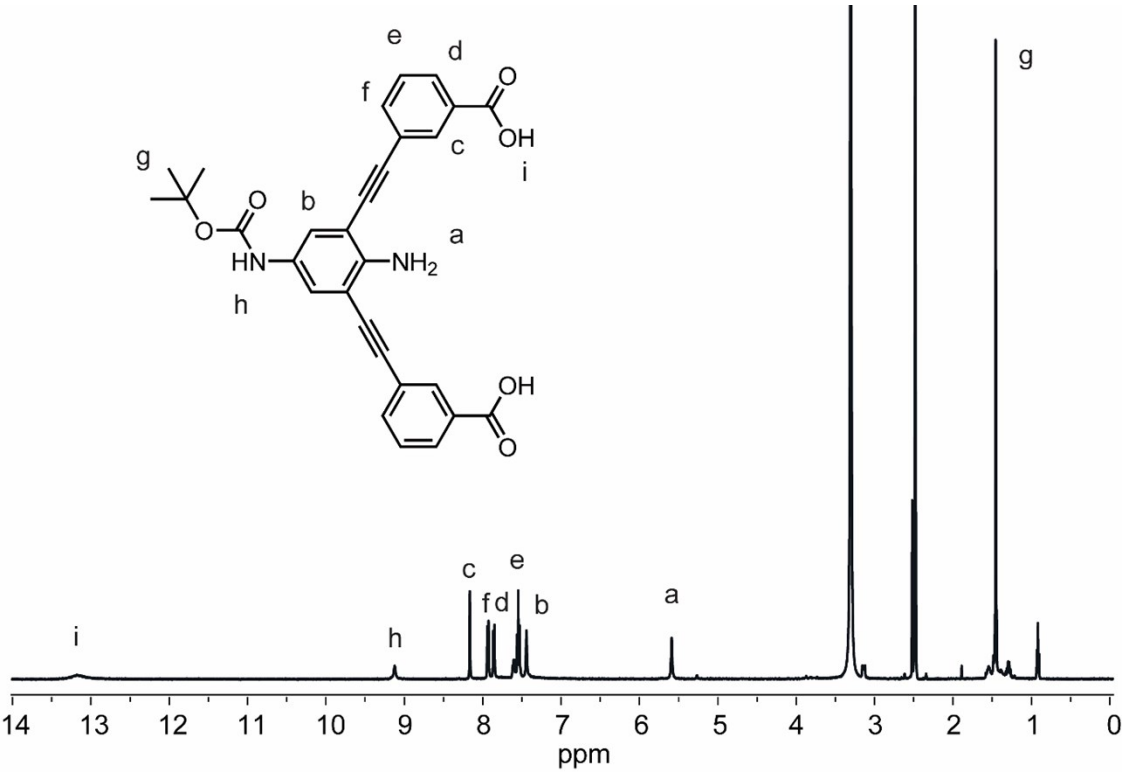

Figure S1. ^{1}H NMR spectrum (DMSO-d_6 / 500 MHz) of **L^2**.

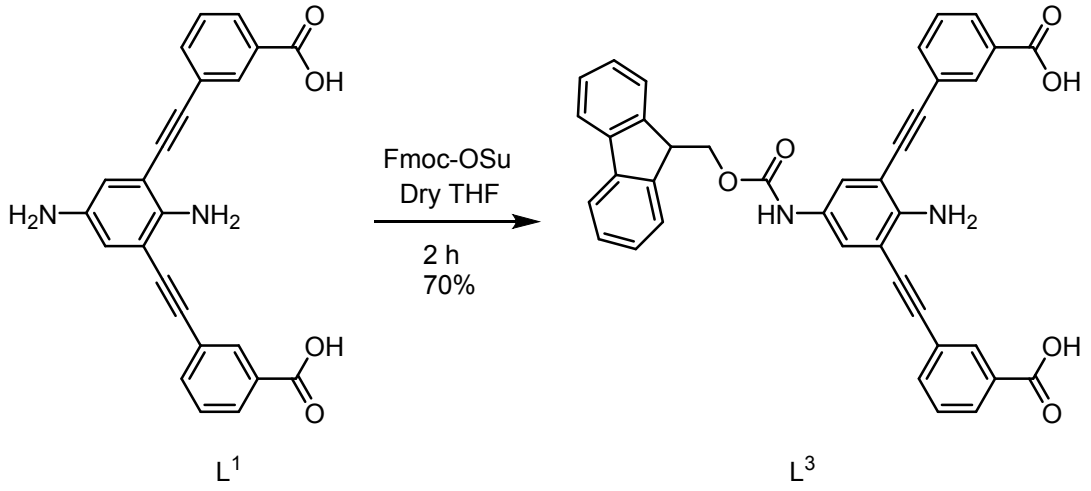

Scheme 3

1.2.7. ***L³***

To a stirred solution of **L¹** (0.500 g, 1.26 mmol) in dry THF (15 mL), N-(9-Fluorenylmethoxycarbonyloxy)succinimide (Fmoc-OSu) (0.468 g, 1.1 eq, 1.38 mmol) was added and the mixture was stirred for 16 h at 25 °C. The solvent was removed under an N_2 stream and MeOH (6 mL) was added. The mixture was acidified to pH = 2 with HCl (2 M) and the resulting precipitate was isolated under reduced pressure, washed extensively with water, and dried under vacuum for 16 h. DMSO (5 mL) and HCl (2 M, 3 mL) were added and the mixture was stirred at 25 °C for 45 minutes. Water (15 mL) was added in one portion and the resulting precipitate was isolated under reduced pressure. Drying the solid under vacuum for 16 h gave 3,3'-((5-((((9H-fluoren-9-yl)methoxy)carbonyl)amino)-2-amino-1,3-phenylene)bis(ethyne-2,1-diyl))dibenzoic acid (**L³**) as a dark green solid (0.540 g, 70%); V_{max} (neat, cm^{-1}): 3425 (w, N-H), 3335 (w), 2968 (w, C-H), 1710 (s, C=O), 1593 (m, C=C), 1433 (m); ^{1}H NMR (500 MHz, DMSO) δ 13.23 (s, 2H, H_i), 9.13 (s, 1H, H_b), 8.18 (s, 2H, H_e), 7.95 (d, *J* = 6.6 Hz, 2H, H_f), 7.86 (d, *J* = 6.6 Hz, 2H, H_f), 7.56 (t, *J* = 7.8 Hz, 2H, H_g), 7.46 (s, 2H, H_c), 5.59 (s, 2H, H_d), 1.47 (s, 9H, H_a); ^{13}C NMR (125 MHz, DMSO) δ175.86, 169.77, 146.90, 143.92, 142.52, 140.55, 138.56, 135.25, 134.50, 132.37,130.80, 128.24, 126.04, 124.50, 123.14, 112.86, 109.18, 96.68, 89.81, 28.34; ESI-MS: calculated for $C_{39}H_{26}N_2O_6$, $[M+H]^+$ 618.1791, found 618.1794.

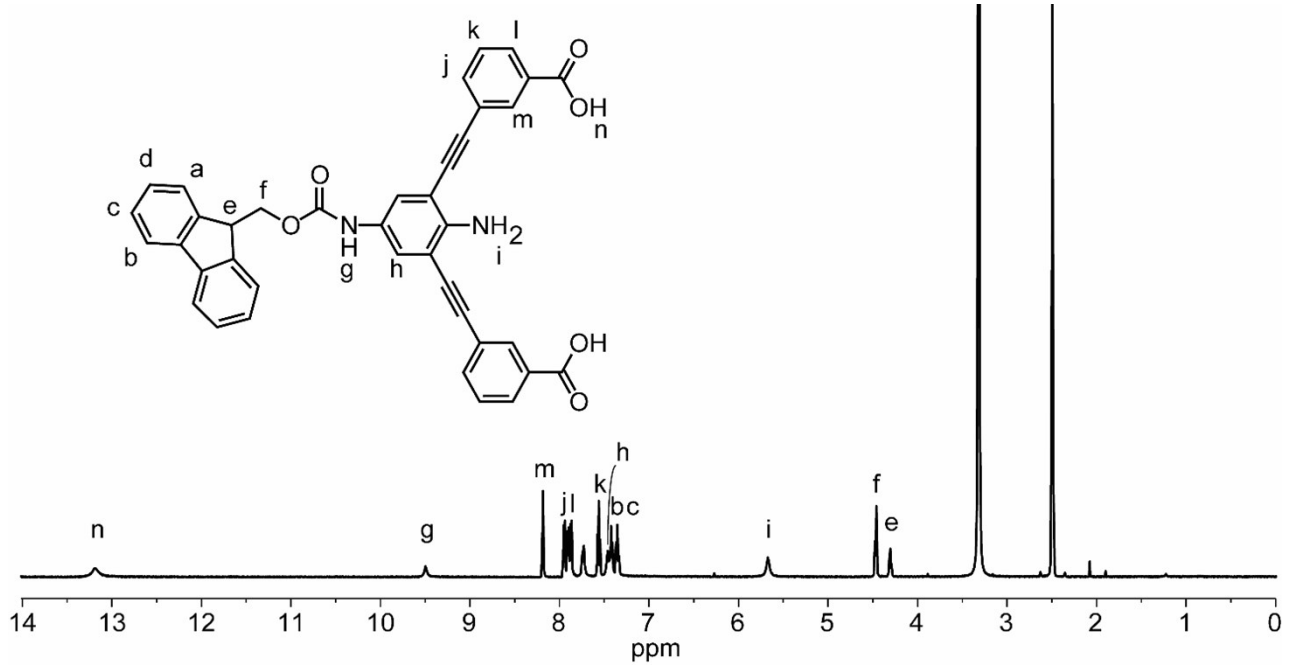

Figure S2. ^{1}H NMR spectrum (DMSO-d_6 / 500 MHz) of **L³**.

1.3. Synthesis of $\{[Cu_x(L^1)_y]\}_n$ (1)

In a screw-cap vial **L¹** (60 mg, 0.15 mmol) was combined with $Cu(OAc)_2 \cdot H_2O$ (40 mg, 0.20 mmol) in 5 mL of (DMSO). A precipitate formed immediately, and the vial was sonicated and left to stand for 1 h at room temperature. The precipitate was collected under reduced pressure, washed with MeOH and dried to afford **1**. ν_{max} (neat, cm^{-1}): 1697.4 (m, HC=O), 1629.3 (m), 1594.9 (m), 1572.8 (m), 1431.3 (m), 1394.9 (s).

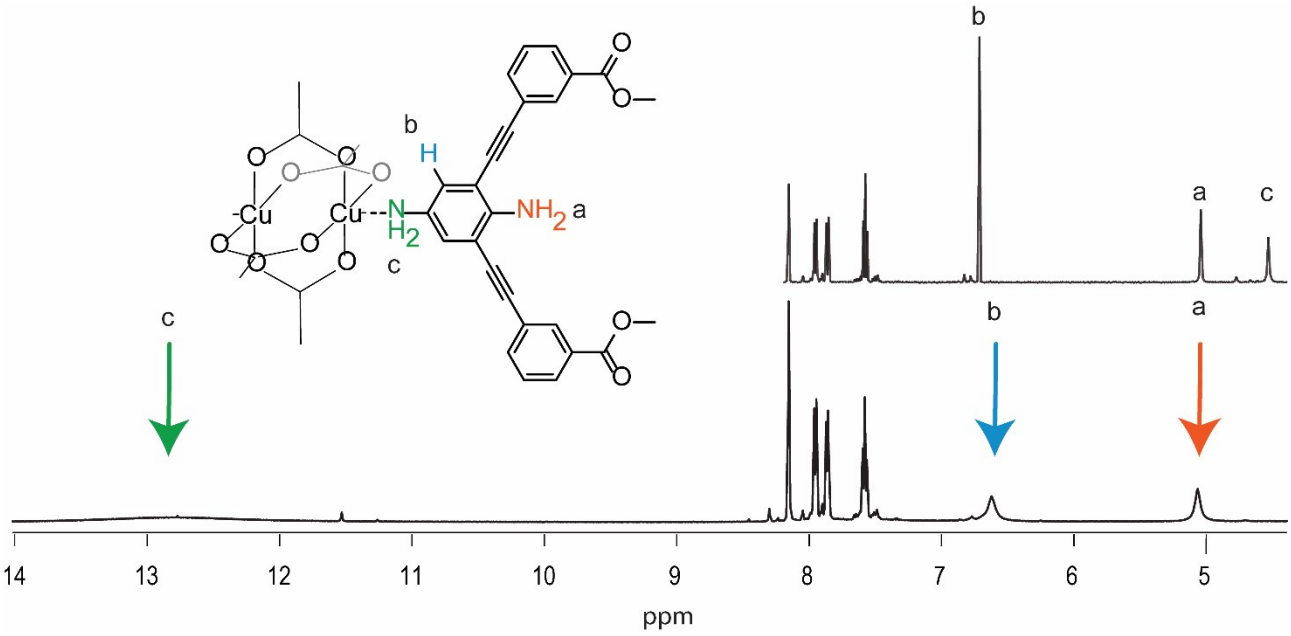

Figure S3. ^1H NMR spectrum (500 MHz/ DMSO-$_{d6}$) of a solution of **L^{1Me}** and $Cu(OAc)_2$ at 25 °C. The shift of proton resonances a, b & c is in agreement with the coordination of the exohedral amine (proton c) to $Cu(OAc)_2$.

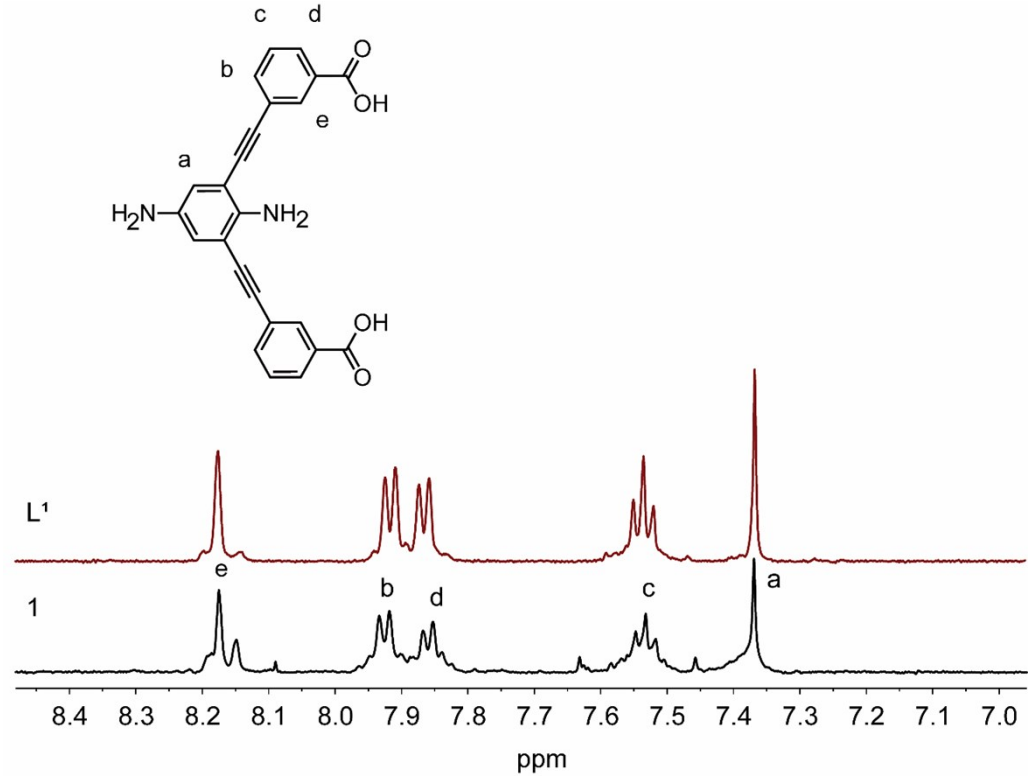

Figure S4. ^1H NMR spectrum (DMSO-d_6 / 500 MHz) of an acid digestion (DCl / DMSO-d_6) of the polymeric material **1**. The signals of the digested polymer are in agreement with **L¹**.

1.4. Synthesis of MOCs

*1.4.1. Synthesis [Cu_4(**L²**)$_4$(solvent)$_4$] (**C^{Boc}**)*

In a screw-cap vial **L²** (5 mg, 0.01 mmol) and copper (II) acetate (3 mg, 0.016 mmol) were combined in DMSO (0.4 mL) and heated at 85 °C for 20 minutes. After removal of any formed solids, a DMSO solution of **2** was obtained. Slow vapour diffusion of methanol into the solution of **C^{Boc}** afforded green rhombohedral crystals after 4 days. The crystals were washed with methanol prior to analysis; V_{max} (neat, cm^{-1}): 3515 – 3111 (br, m, MeOH (O-H)), 2928 (w, C-H), 1714 (s, C=O), 1659 (m), 1621 (m), 1591 (m, C=C), 1569 (m), 1391 (s). Found: C 57.74 H 4.394 N 4.67 $C_{116}H_{120}Cu_4N_8O_{40}$ requires: C 58.21 H 5.05 N 4.68.

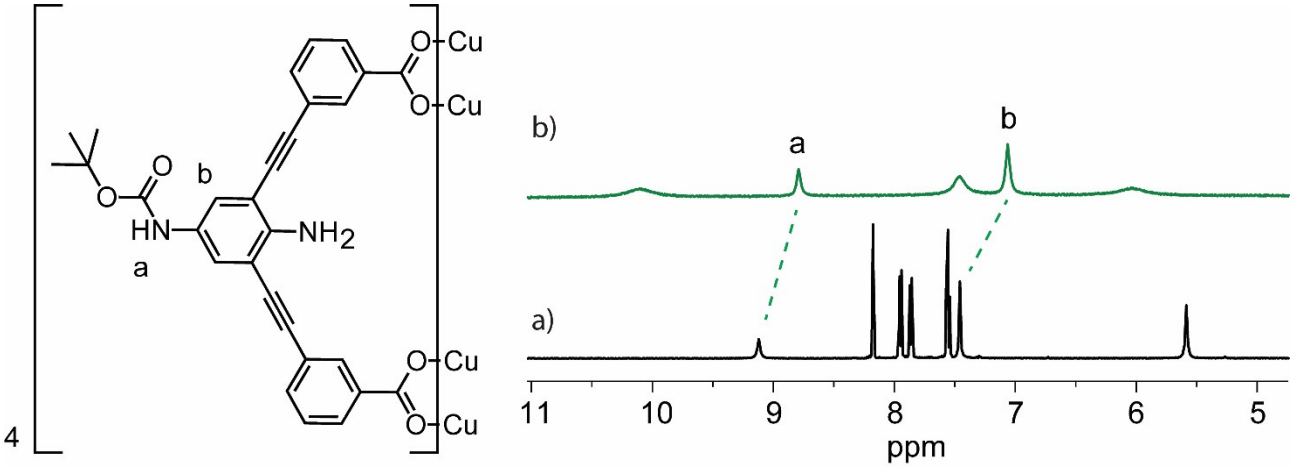

Figure S5. ^{1}H NMR spectrum (DMSO-d_6 / 500 MHz) of a) **L²** and b) **L²** after the addition of $Cu(OAc)_2$ (**C^{Boc}**).

*1.4.2. Synthesis of [Cu_4(**L³**)$_4$(solvent)$_4$] (**C^{Fmoc}**)*

In a screw-cap vial **L³** (5 mg, 0.01 mmol) and copper (II) acetate (3 mg, 0.016 mmol) were combined in DMF (0.4 mL) and heated at 60 °C for 15 minutes. After removal of the precipitate by-product, a DMF solution of **C^{Fmoc}** was obtained. Slow vapour diffusion of methanol into the solution of **C^{Fmoc}** afforded green rhombohedral crystals after 4 days. The crystals were washed with methanol prior to analysis; V_{max} (neat, cm^{-1}): 2927 (w, C-H), 1699 (s, C=O), 1621 (m), 1591 (C=C), 1429 (m), 1394 (s). Found: C 61.36 H 4.12 N 3.64 $C_{156}H_{132}Cu_4N_8O_{42}$ requires: C 61.53 H 4.37 N 3.68.

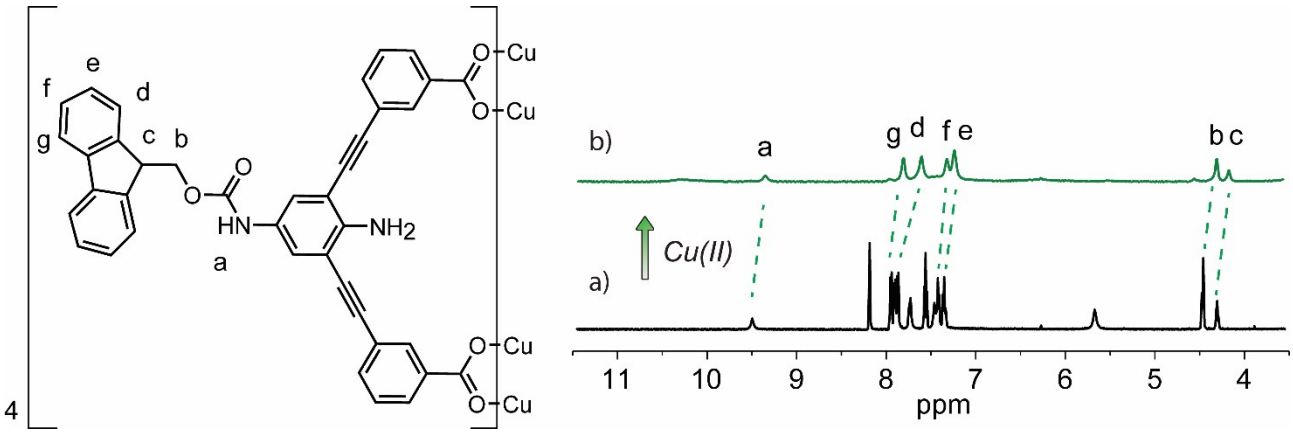

Figure S6. ^{1}H NMR spectrum (DMSO-d_6 / 500 MHz) of a) **L³** and b) **C^{Fmoc}**.

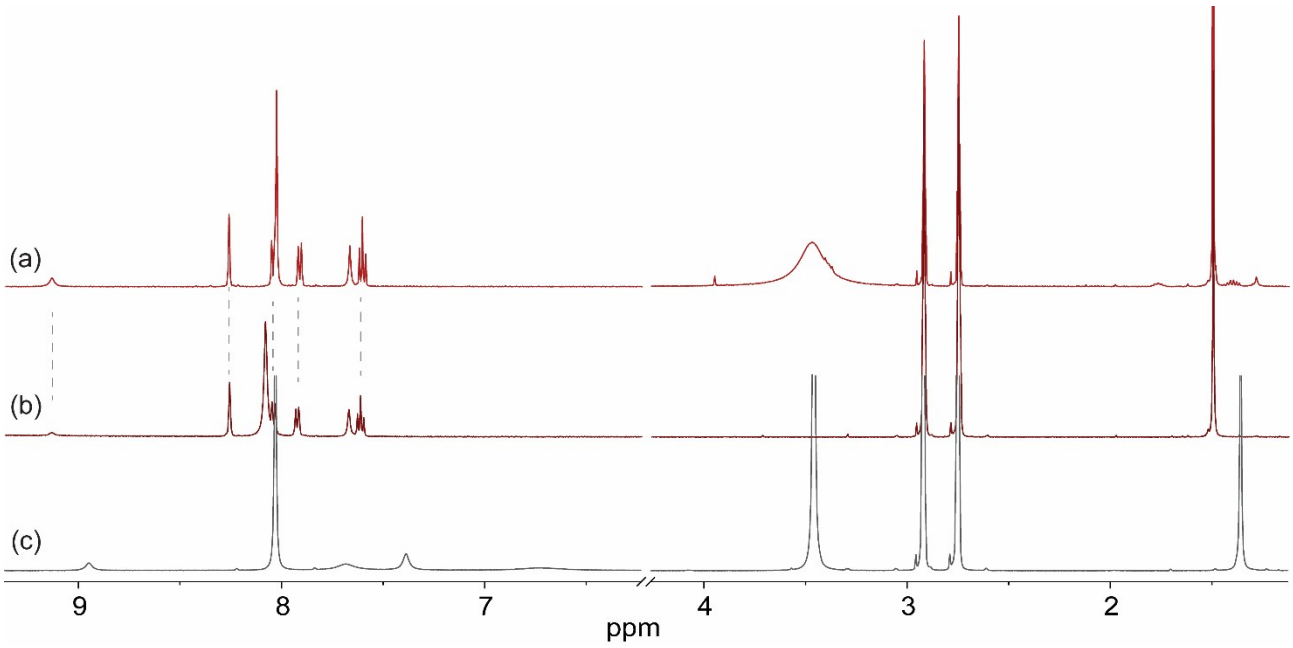

Figure S7. ^{1}H NMR (500 MHz / DMF-d_7) spectra showing an attempt to deprotect $\mathbf{C^{Boc}}$ with trifluoro acetic acid (TFA). The spectra indicate complete disassembly of the cage under these conditions: (a) $\mathbf{L^2}$, (b) $\mathbf{C^{Boc}}$ + TFA and (c) $\mathbf{C^{Boc}}$.

2. UV-Vis & Fluorescence spectroscopy

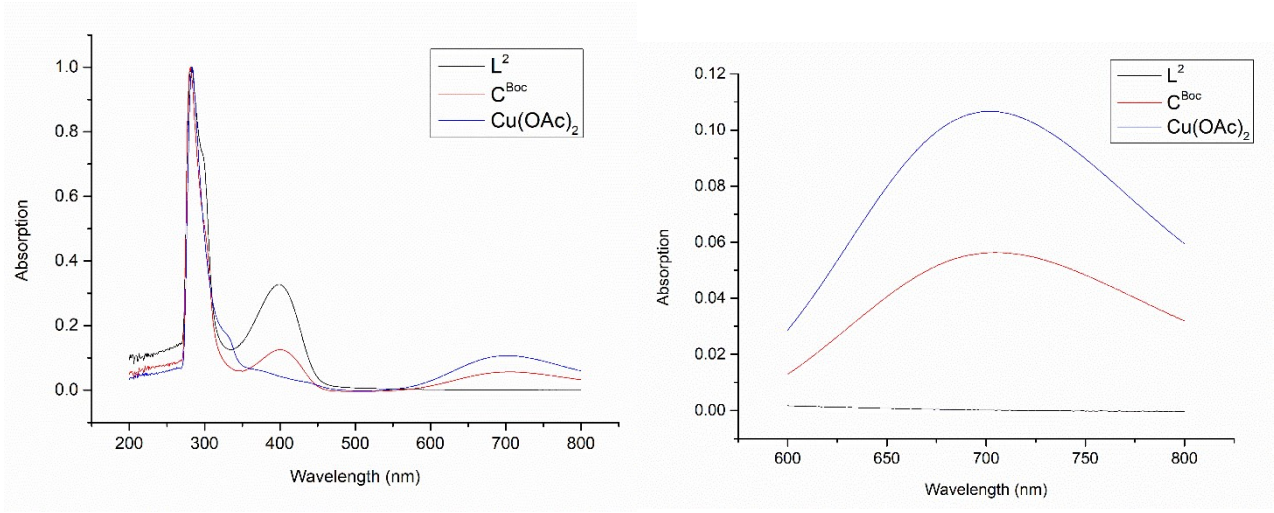

Figure S8. UV-Vis spectrum of $\mathbf{L^2}$, $\mathbf{C^{Boc}}$ and $\mathbf{Cu(OAc)_2}$ in DMSO indicating formation of the cage species $\mathbf{C^{Boc}}$ in solution. Shifting of the maxima absorption peak in the copper paddlewheel region (600 – 800) is consistent with the formation of the desired Cu_4L_4 copper paddlewheel cage.[4]

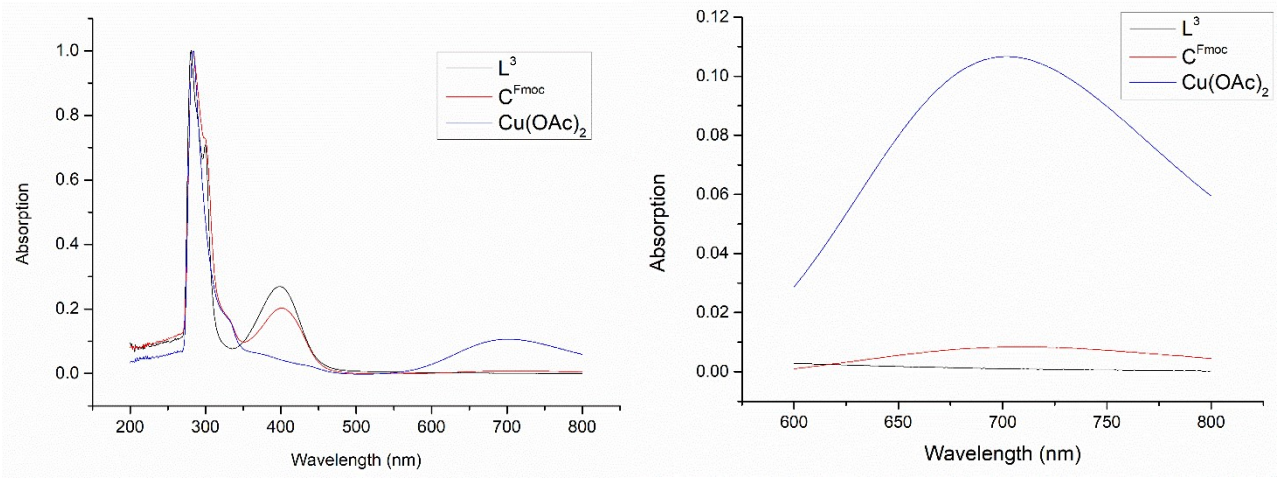

Figure S9. UV-Vis spectrum of **L³**, **C^{Fmoc}**, and **Cu(OAc)$_2$** in DMF indicating formation of the cage species **C^{Fmoc}** in solution. Shifting of the maxima absorption peak in the copper paddlewheel region (600 – 800) is consistent with the formation of the desired Cu_4L_4 copper paddlewheel cage.[4]

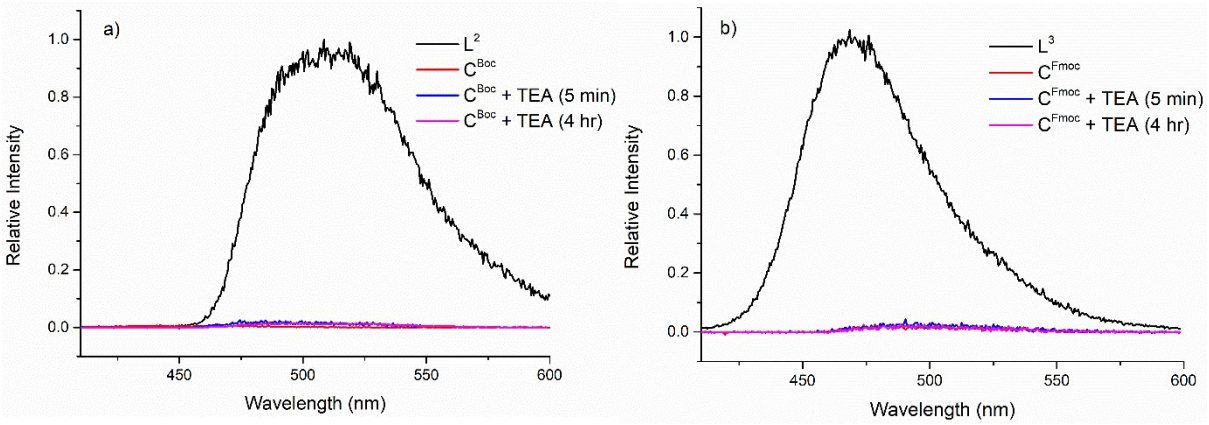

Figure S10. a) Fluorescence spectra of **L²** (0.0059 mM, black), **C^{Boc}** (0.26 mM, red), **C^{Boc}** + TEA (10%, 5 min, blue) and **C^{Boc}** + TEA (10 %, 4 hr, pink). b) Fluorescence spectra of **L³** (0.0048 mM, black), **C^{Fmoc}** (0.21 mM, red), **C^{Fmoc}** + TEA (10%, 5 min, blue) and **C^{Fmoc}** + TEA (10%, 4 hr, pink). Both sets of spectra clearly indicate that addition of TEA does not result in an increase in fluorescence (that would otherwise be attributed release of free ligand/cage disassembly).

2.1. Synthesis of SCPs 2a-c

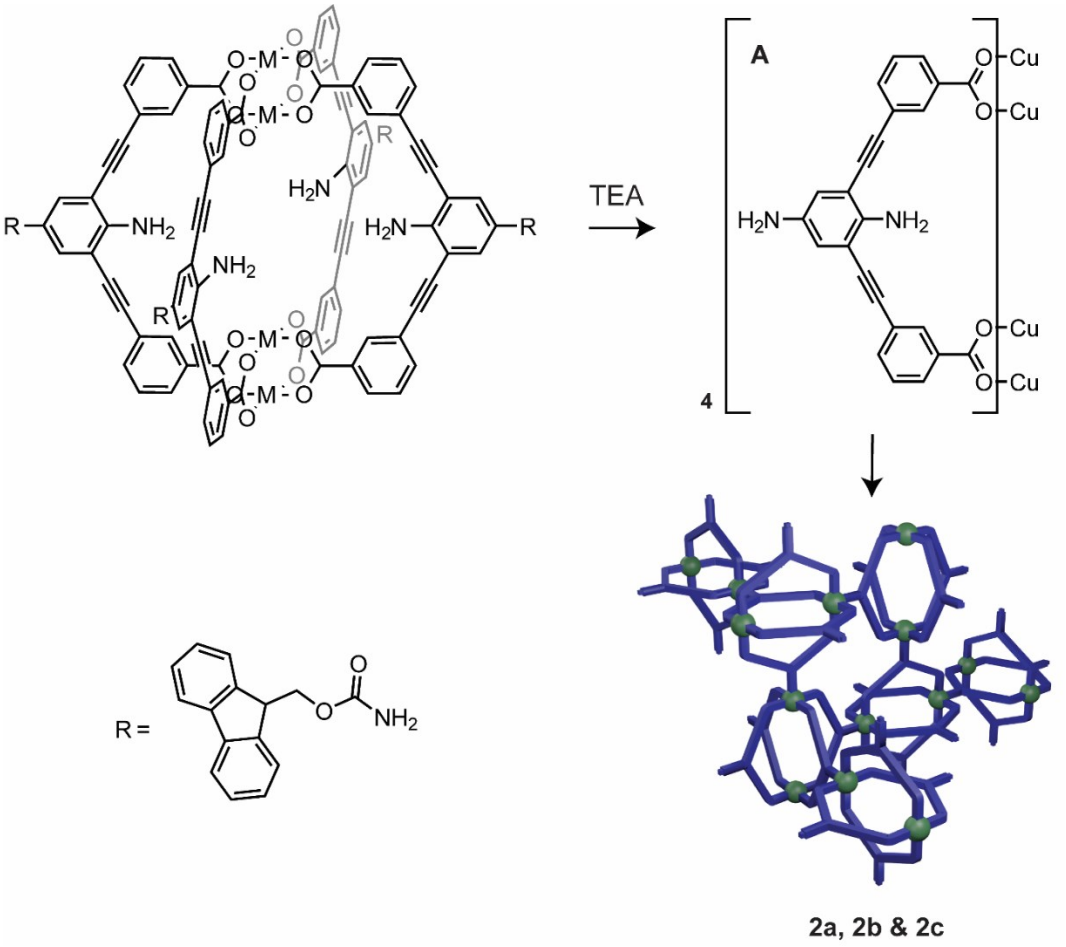

Figure S11. A scheme depicting the deprotection of $[Cu_4L^3_4(solvent)_4]$ ($\mathbf{C^{Fmoc}}$) and subsequent assembly of SCPs **2a-c**. Since proton resonances corresponding to L^3 are not observed in the acid digestion of **2a-c**, we propose that a free amine cage, denoted **A**, exists transiently in solution before polymerisation occurs.

*2.1.1. Fmoc deprotection of $[Cu_4(L^3)_4(MeOH)_4]$ (C^{Fmoc}); synthesis of **2a-c***

In a screw-cap vial, DMF (0.5 mL) was added to $\mathbf{C^{Fmoc}}$ (6 mg, 0.0022 mmol). After removal of undissolved solids, TEA (30 µL) was added in one portion. After standing at room temperature for 3 h, an amorphous precipitate was formed. The precipitate was collected, washed with MeOH to remove the expected deprotection by-products and dried under vacuum to afford **2a**. ν_{max} (neat, cm^{-1}): 1703 (m), 1611 (m), 1544 (m), 1423 (m), 1394 (m). Found: C 54.82 H 4.16 N 4.50 $C_{100}H_{100}Cu_4N_8O_{34}$ requires: C 54.30 H 4.16 N 4.50. **2b** and **2c** were prepared in a similar manner, albeit with 50 µL: and 100 µL: of TEA respectively. **2b**: Found: C 50.73 H 3.38 N 5.21 $C_{96}H_{102}Cu_4N_8O_{39}$ requires: C 51.34 H 4.58 N 4.99. **2c**: Found: C 50.60 H 3.39 N 5.29 $C_{96}H_{104}Cu_4N_8O_{40}$ requires: C 50.93 H 4.63 N 4.95

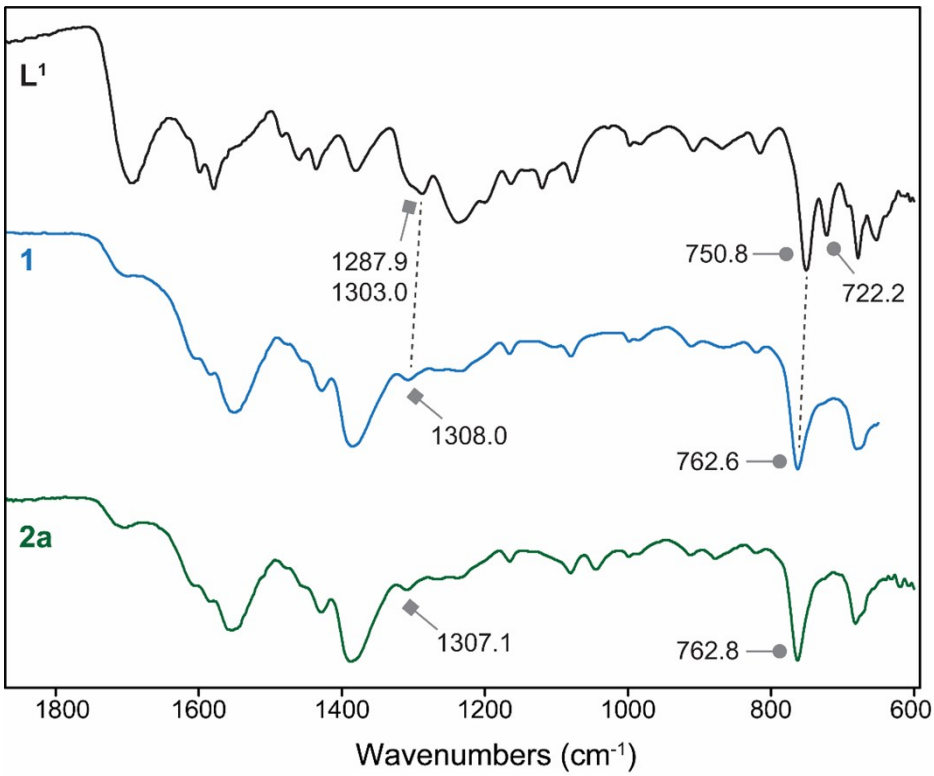

Figure S12. IR spectrum (neat) of **L¹**, **1** and **2a**. The NH_2 wags (from the phenylene diamine core) occur at 750.8 cm-1 and 722.2 cm^{-1}. Only a single NH_2 wag is observed for **1** and **2a-c** at ~ 762 cm^{-1}, which is consistent with the coordination of one of the NH_2 donors to Cu(II).

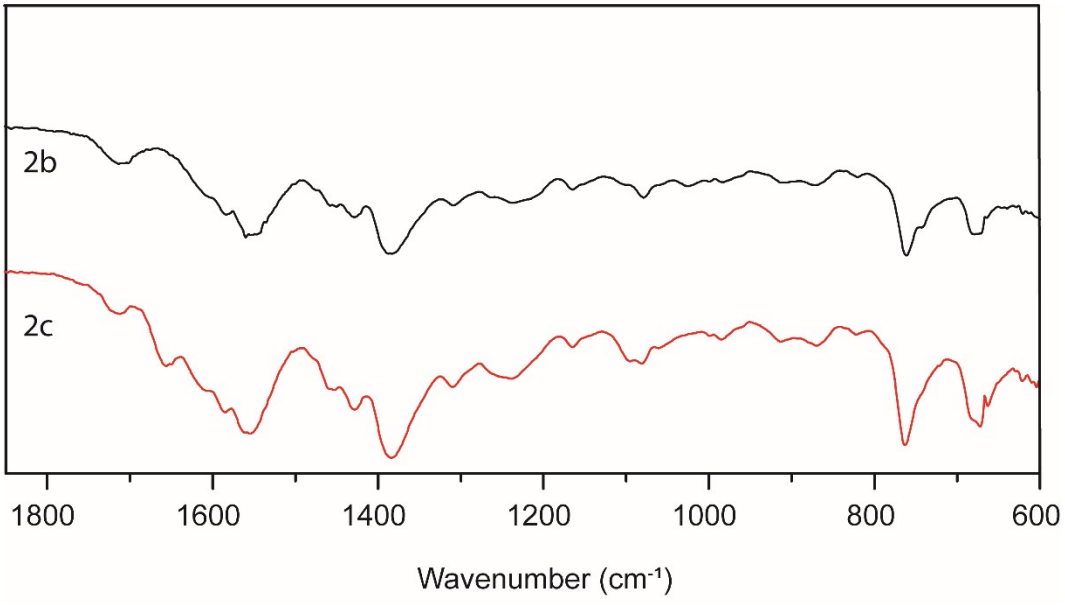

Figure S13. IR spectra (neat) of **2b** and **2c**.

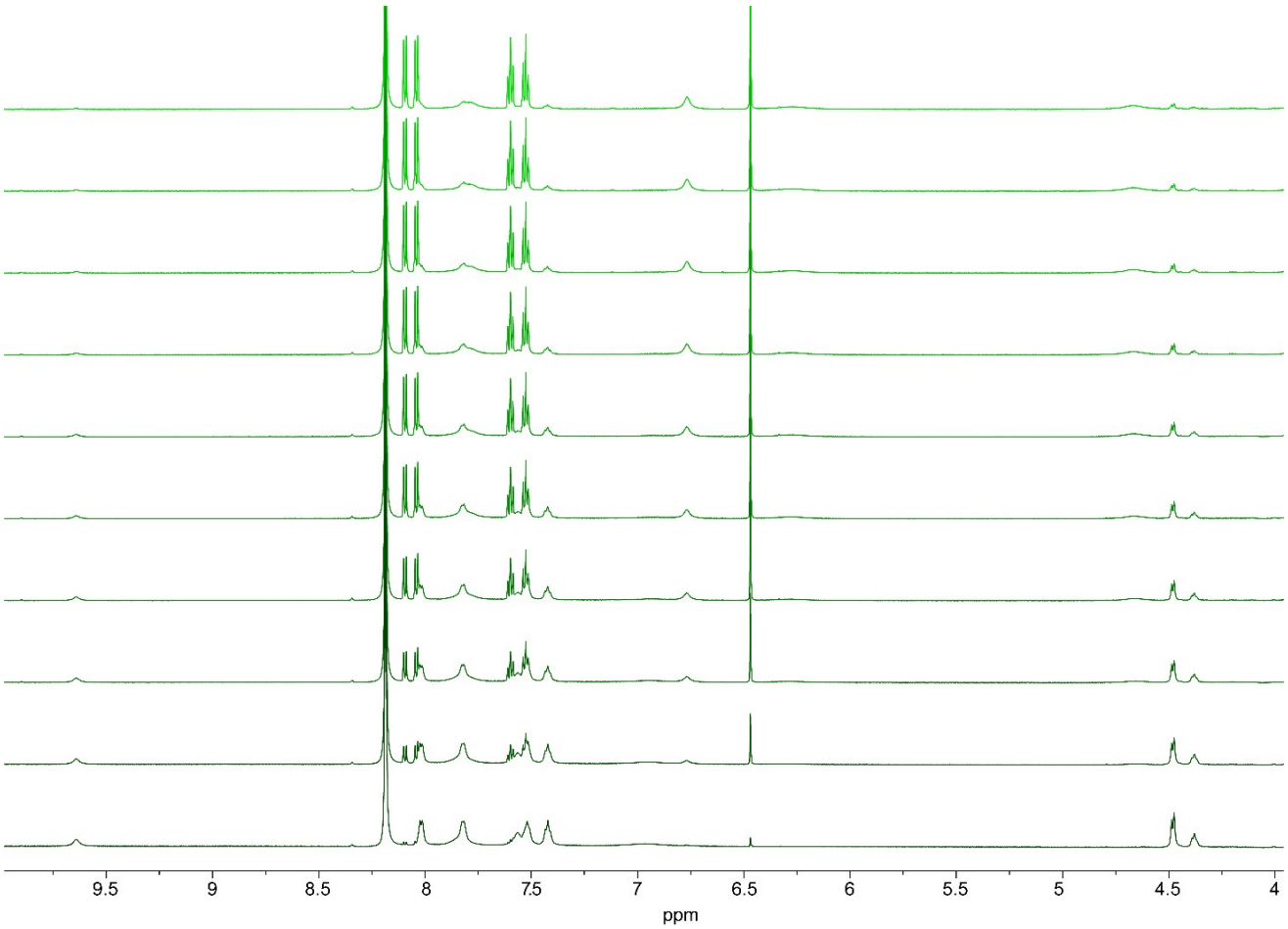

Figure S14. ^{1}H NMR array experiment following the deprotection of Fmoc from $\mathbf{C}^{\mathbf{Fmoc}}$ with TEA. The above figure represents 40 min intervals between each spectra from bottom to top. Proton resonances relating directly to the expected DBF (dibenzofulvene) by-product are observed with the disappearance of broad resonances relating to $\mathbf{C}^{\mathbf{Fmoc}}$. Allowing the reaction to sit for a further 3 hrs did not reveal any changes in the collected ^{1}H NMR spectrum.

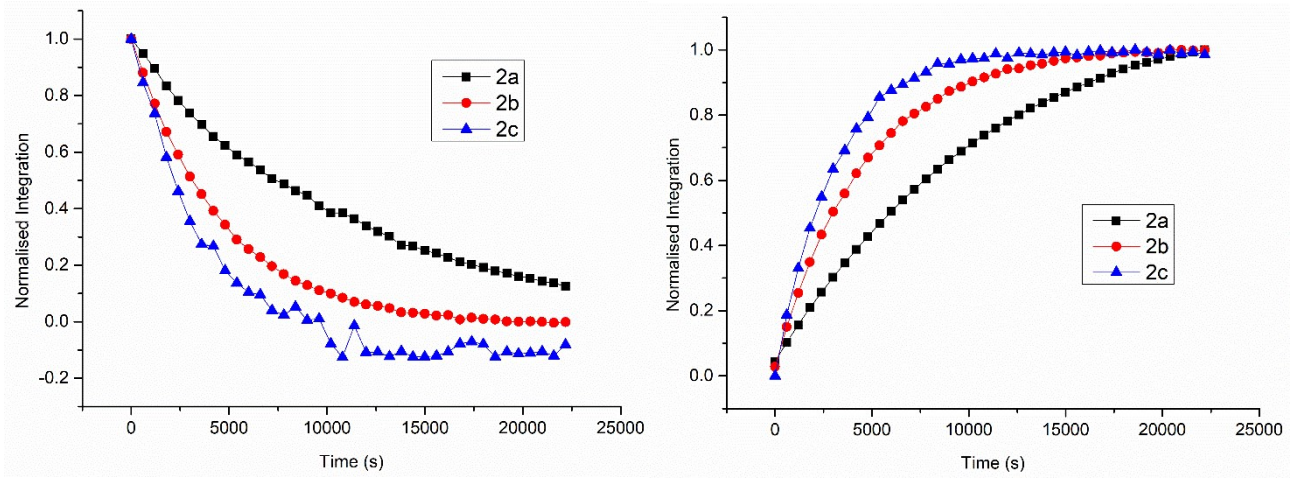

Figure S15. Integration data from the ^{1}H NMR spectroscopy array experiment, examining the deprotection of $\mathbf{C}^{\mathbf{Fmoc}}$. From the array data, it is clear that the deprotection occurs at a faster rate with increasing quantities of triethylamine (TEA; black = 30 µL, red = 50 µL, blue = 100 µL). The plot on the left shows the decrease in signal intensity of the Fmoc protecting group aromatic resonance of $\mathbf{C}^{\mathbf{Fmoc}}$. The plot on the right indicates the evolution of the expected dibenzofulvene (DBF) by-product as a result of deprotection.

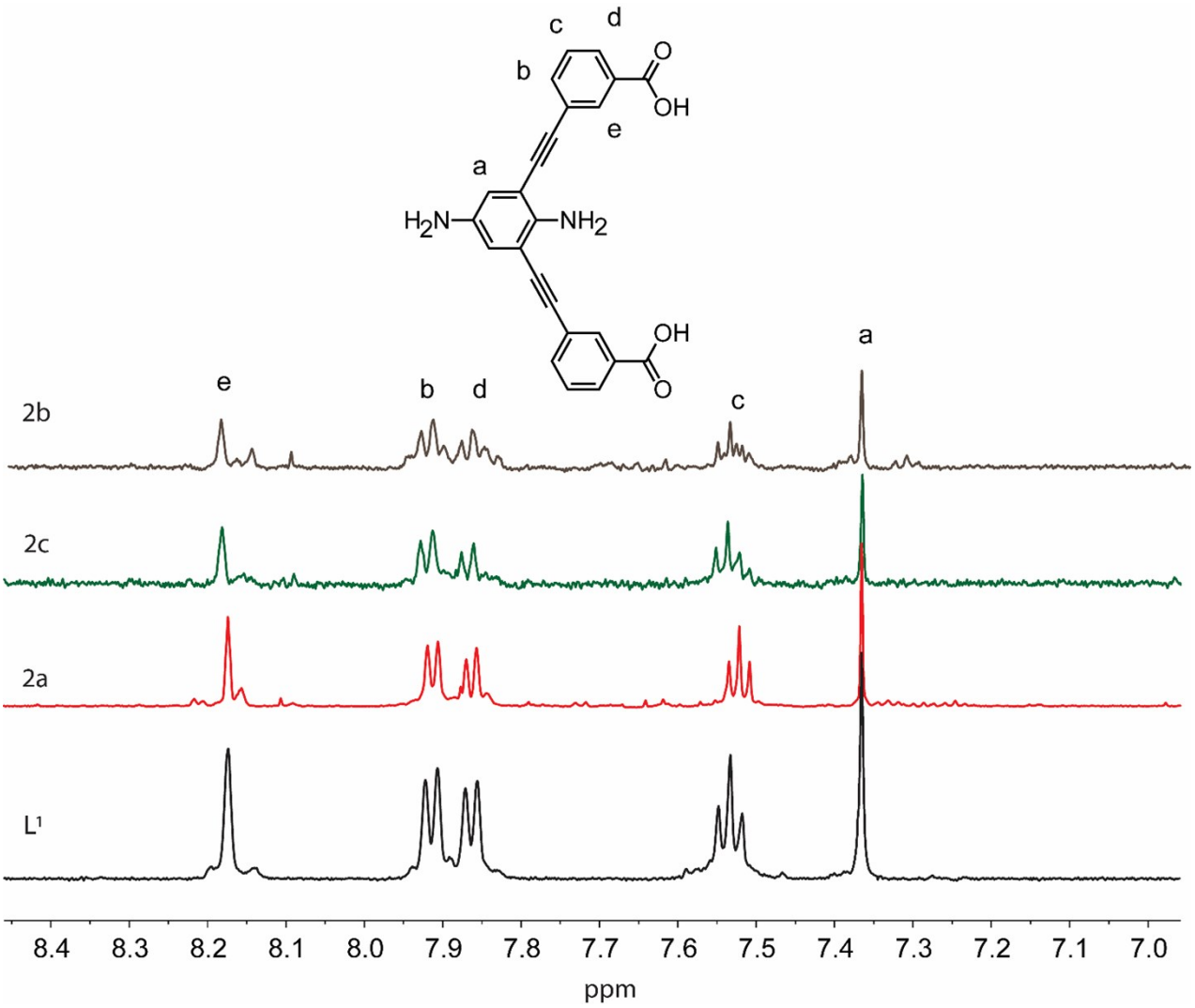

Figure S16. ^{1}H NMR (DMSO-d_6 / 500 MHz) spectra of acid digested samples (**2a**, **2b** & **2c**) formed by the deprotection of $\mathbf{C^{Fmoc}}$ with TEA. Proton resonances associated with $\mathbf{L^{1}}$ are evident in the spectra of all deprotected materials. * is the shifted H_2O peak due to the addition of DCl.

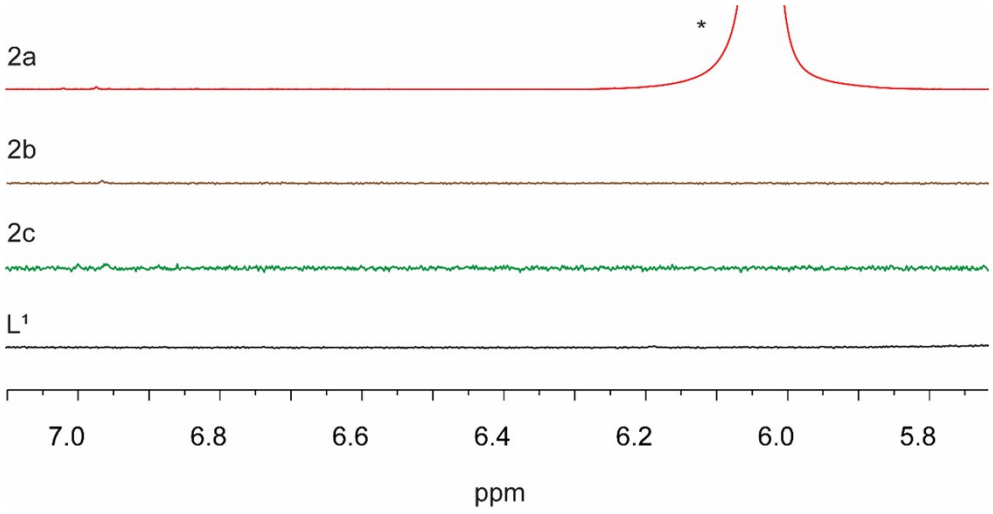

Figure S17. ^{1}H NMR (DMSO-d_6 / 500 MHz) spectra of acid digested samples (**2a**, **2b** & **2c**) formed by the deprotection of $\mathbf{C^{Fmoc}}$ with TEA. The ^{1}H NMR highlights the characteristic region for the olefinic protons of the dibenzofulvene (DBF) by product. These spectra indicate that the DBF has been removed during the activation process. * represents the shifted H_2O signal due to the addition of DCl.

3. Powder X-ray diffraction (PXRD)

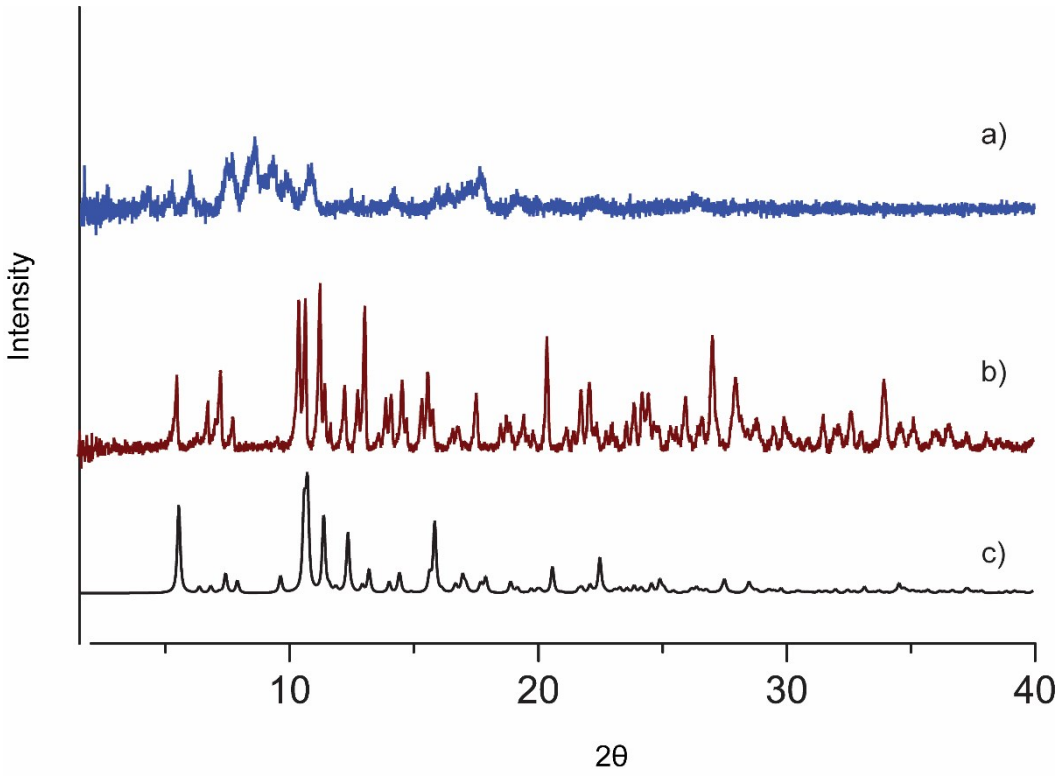

Figure S18. Powder X-ray diffraction patterns of $\mathbf{C}^{\mathbf{Fmoc}}$ of a) activated, b) as-synthesised and c) simulated from single-crystal X-ray data.

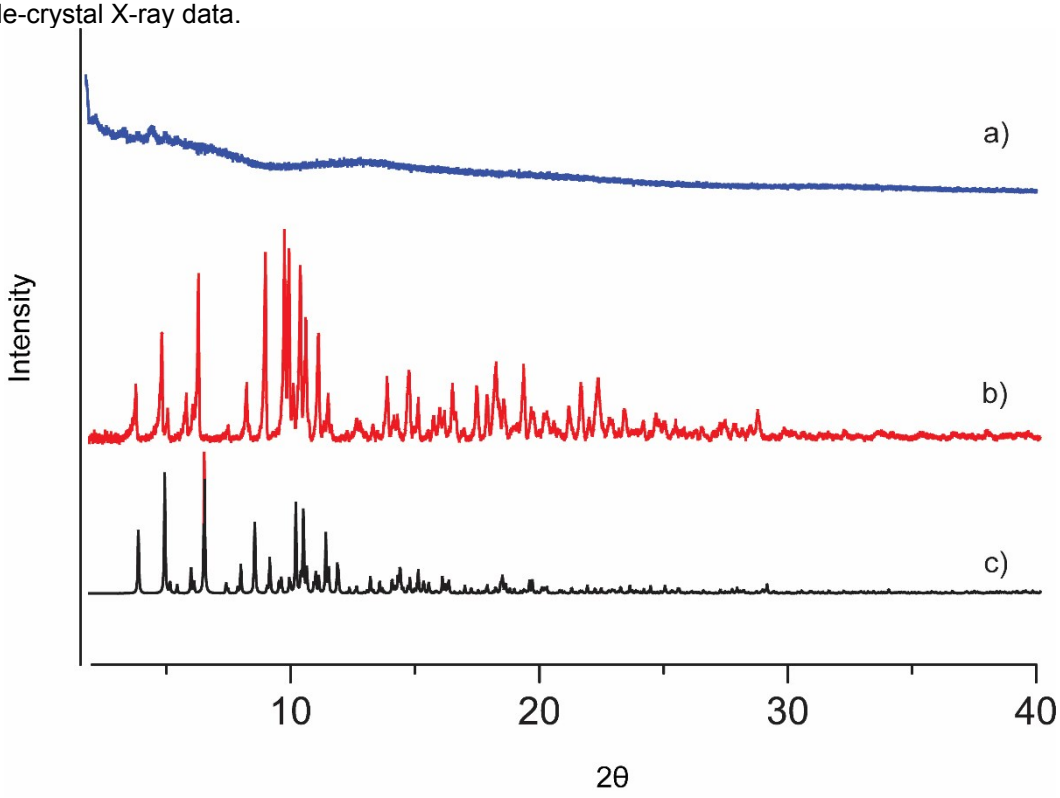

Figure S19. Powder X-ray diffraction patterns of $\mathbf{C}^{\mathbf{Boc}}$ a) activated, b) as-synthesised and c) simulated from single-crystal X-ray data.

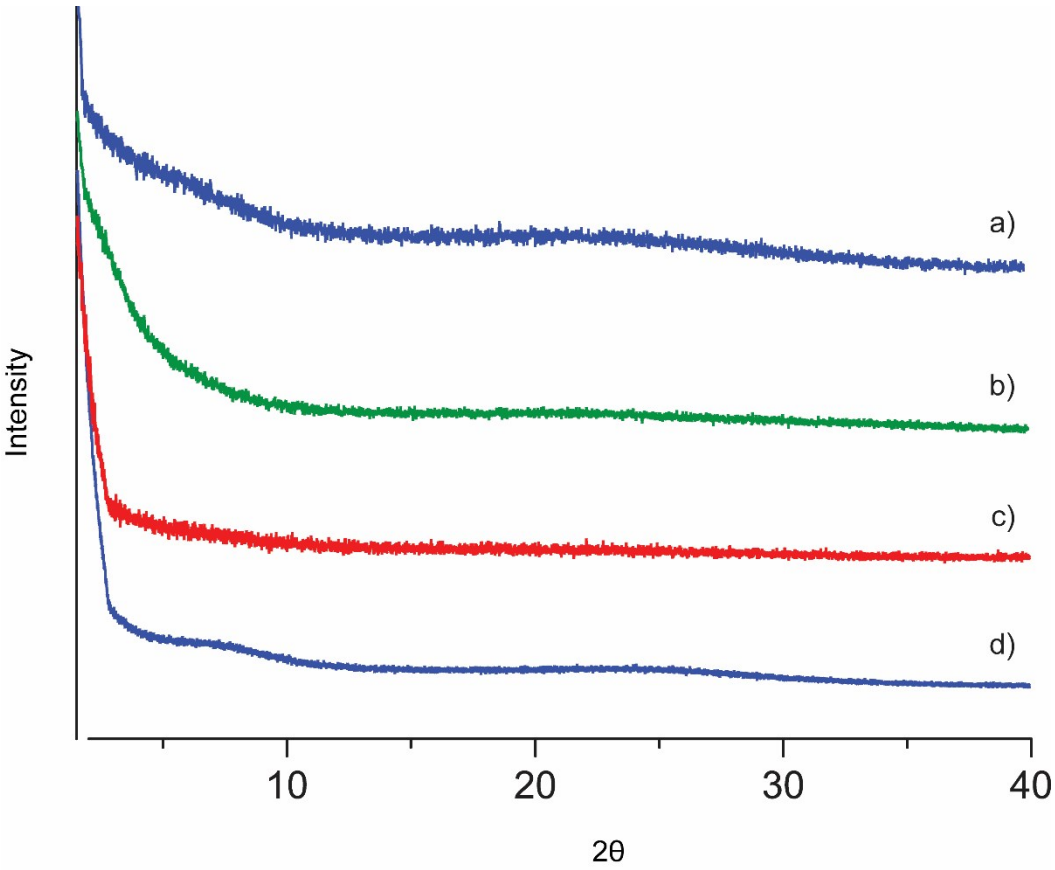

Figure S20. Powder X-ray diffraction patterns confirming the amorphous character of a) **2c**, b) **2b**, c) **2a** and d) **1**.

4. Thermal gravimetric analysis (TGA)

Note: Figures S19 and S20 shows the TGA and RGA data of our initial attempts to monitor the deprotection of $\mathbf{C^{Boc}}$ via thermolysis. The production of isobutylene as evident by the evolution of isobutylene (RGA trace) suggests that thermal deprotection of Boc is occurring at elevated temperatures. However, due to the reactivity of free amines in the presence of copper at these temperatures[5], the samples underwent complete decomposition >100 °C.

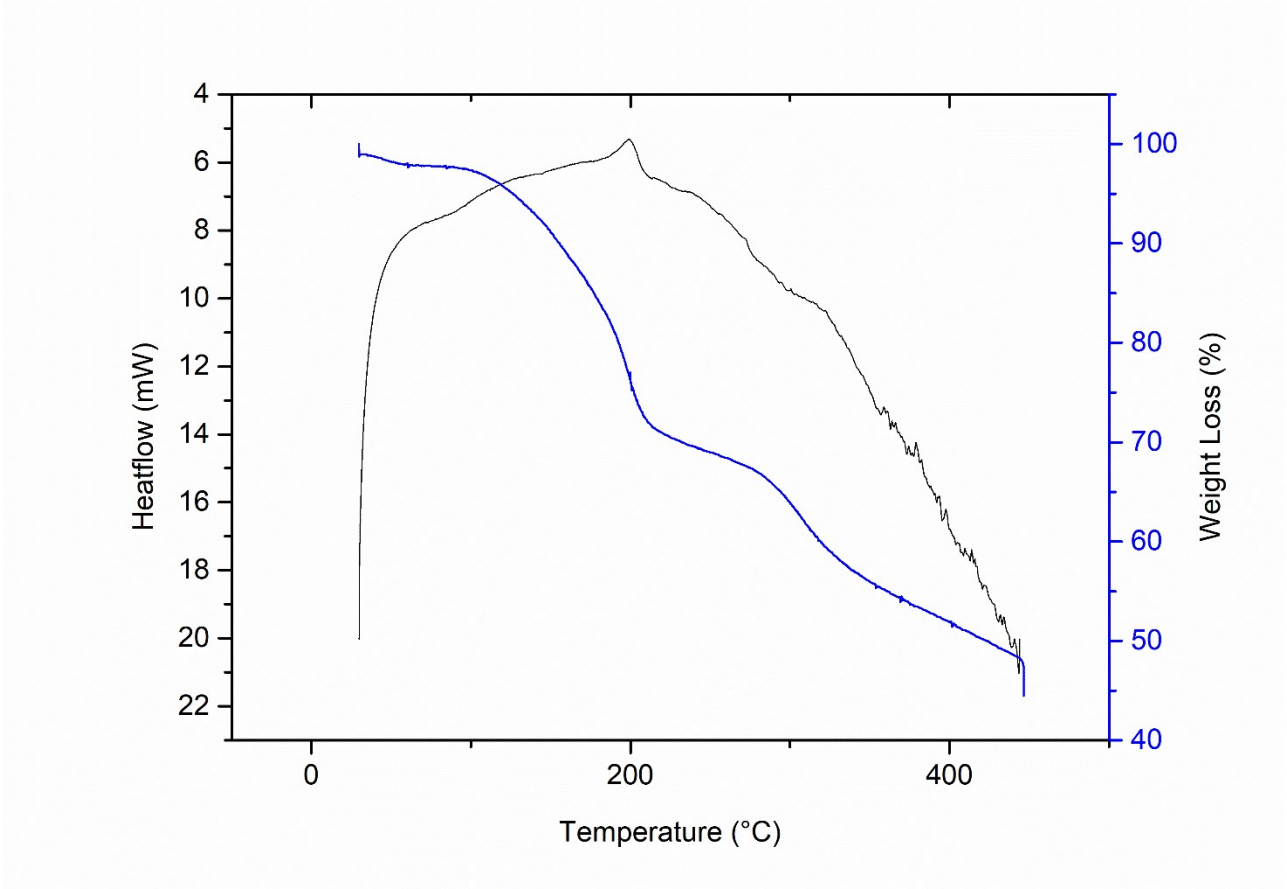

Figure S21. TGA-DSC trace of the solid sample of $\mathbf{C^{Boc}}$ (blue line = % weight loss, black line = DSC trace).

Table S1: Calculated weight loss of the expected by products of Boc deprotection and coordinated MeOH solvent ligands compared to the total observed experimental weight loss.

Theoretical Weight Loss		**Observed Weight Loss**
MeOH (solvent)	5.6 %	
Boc by-products	18%	
Total = 23.6%		**Total = 25%**

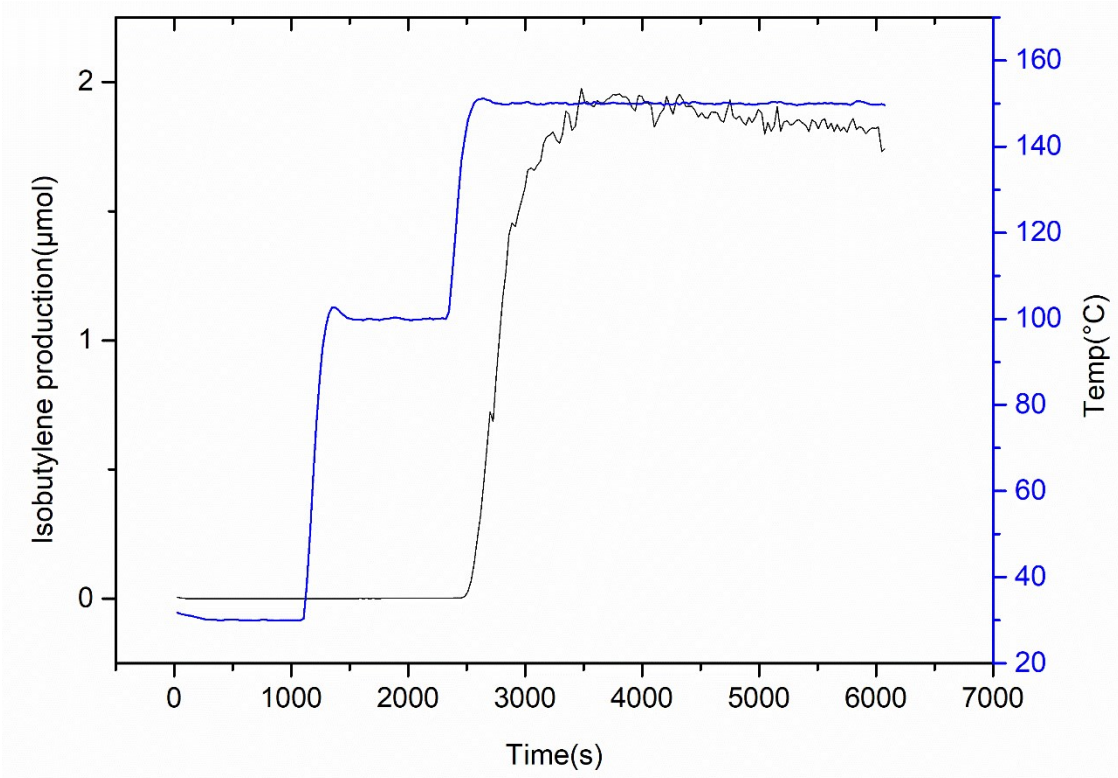

Figure S22. RGA graph of the Boc thermolysis reaction of $\mathbf{C}^{\mathbf{Boc}}$ indicating the evolution of isobutylene (black curve) according to temperature (blue line).

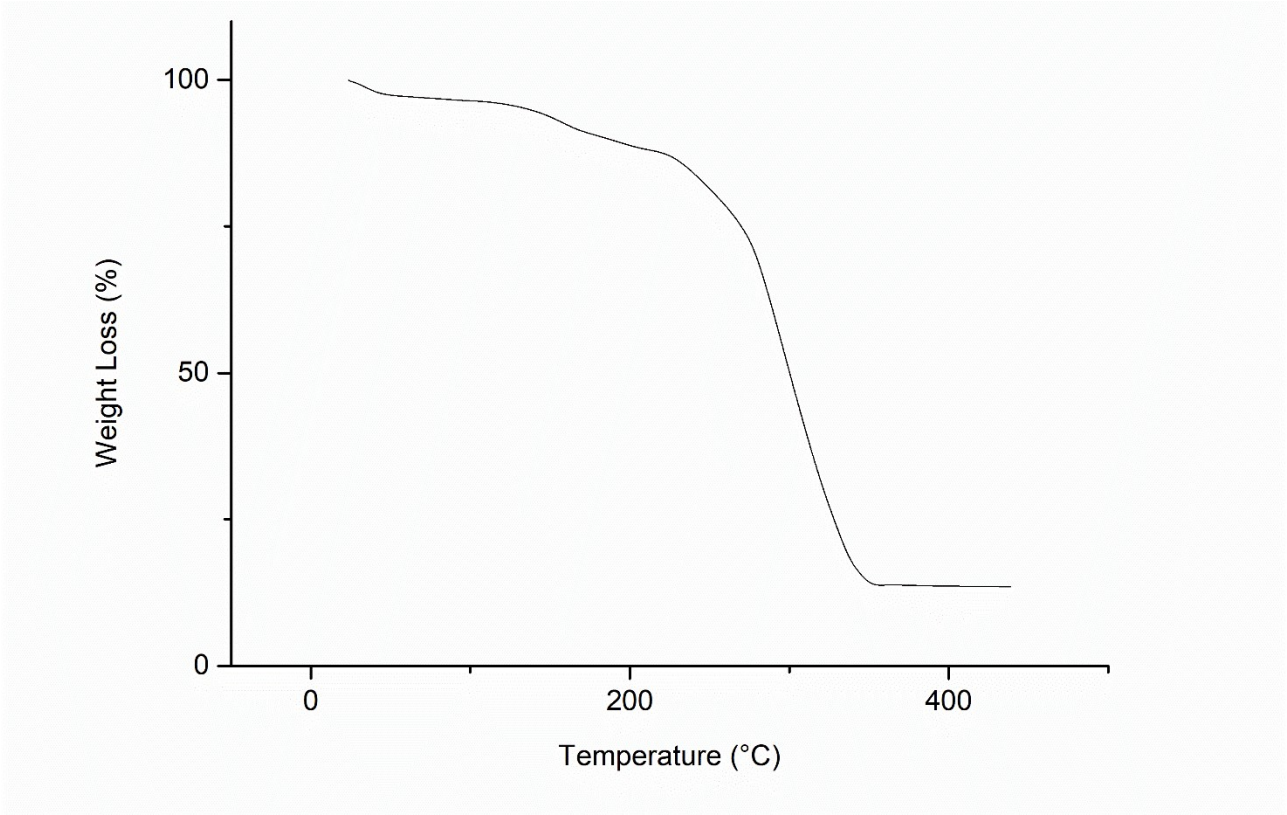

Figure S23. TGA trace of $\mathbf{C}^{\mathbf{Fmoc}}$**.** A solvent weight loss of 12.5% is apparent between 30 – 220 °C, which is followed by decomposition ~ 220 °C

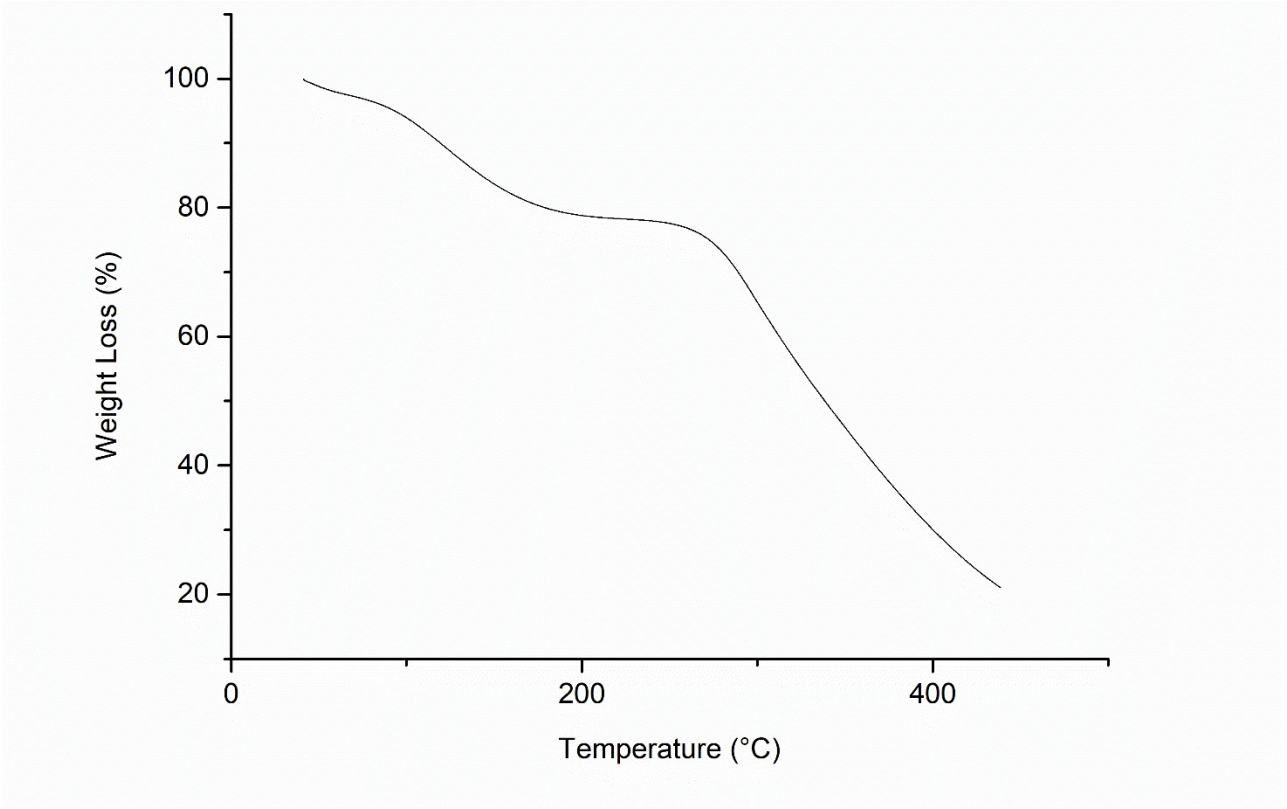

Figure S24. TGA trace of **1**. A solvent weight loss of 10.4% is apparent between 30 – 250 °C with decomposition occurring at 270 °C

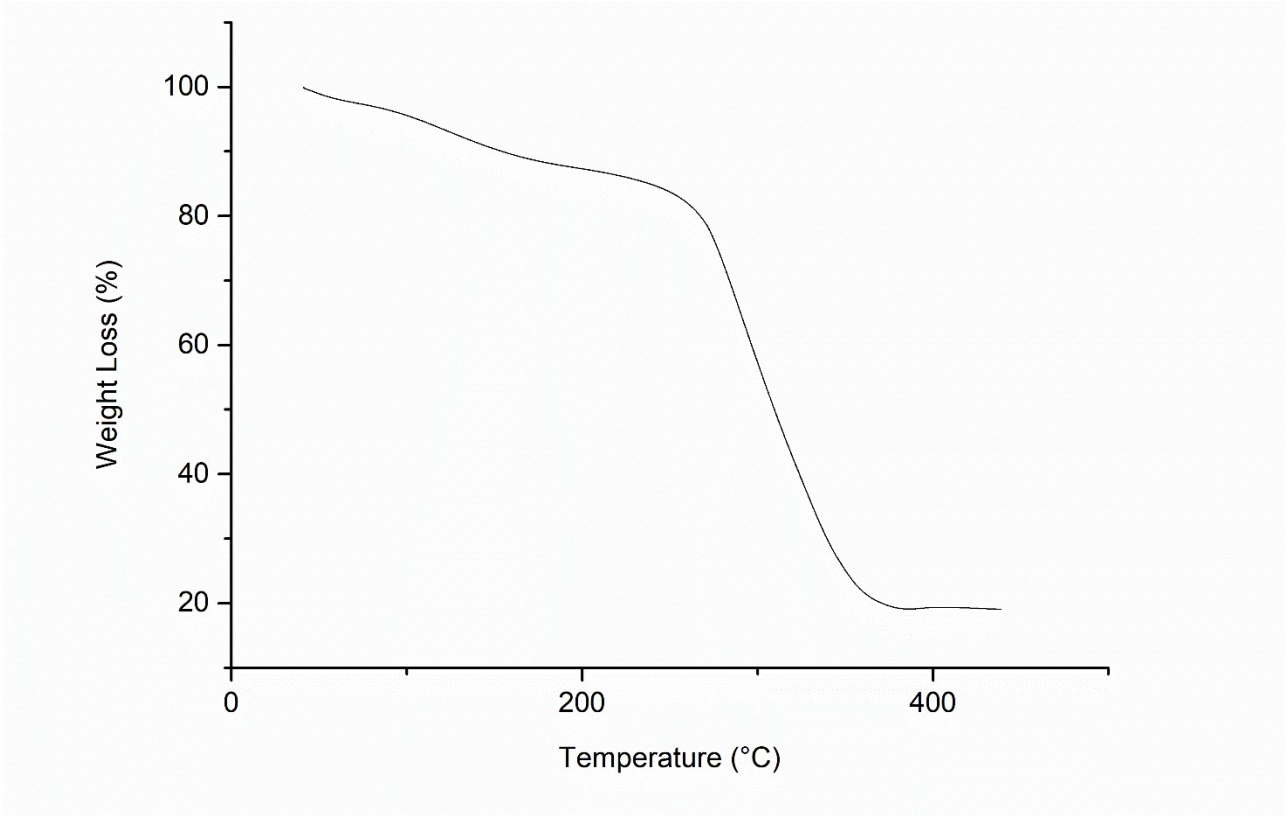

Figure S25. TGA trace of **2a**. A solvent weight loss of 9% is apparent between 30 – 260 °C with decomposition occurring at 260 °C

5. Gas adsorption

1, 2a, 2b, 2c & **C^{Fmoc}** were washed with diethyl ether (x 4) over 12 hours followed by pentane exchange over a two-hour period. All samples activated under high vacuum for 3 hours prior to the experiment commencement.

C^{Boc} was activated via exchanging the solvent with MeOH followed by exposure to a high vacuum overnight at 60 °C.

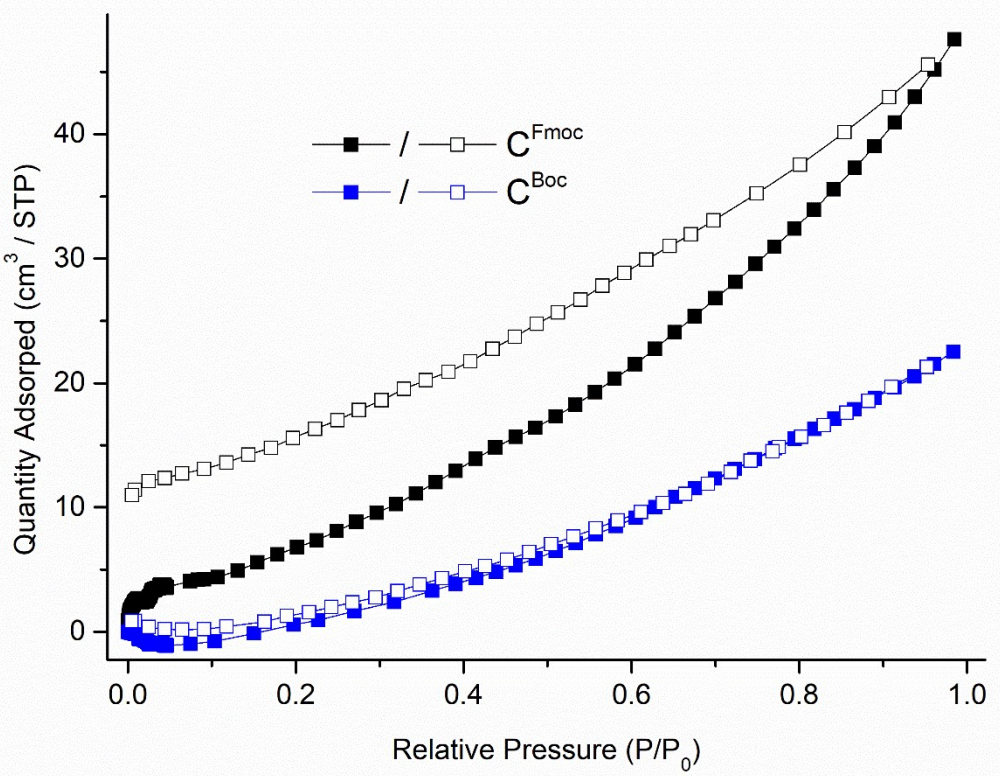

Figure S26. 77k N_2 adsorption isotherm of **C^{Boc}** & **C^{Fmoc}**.

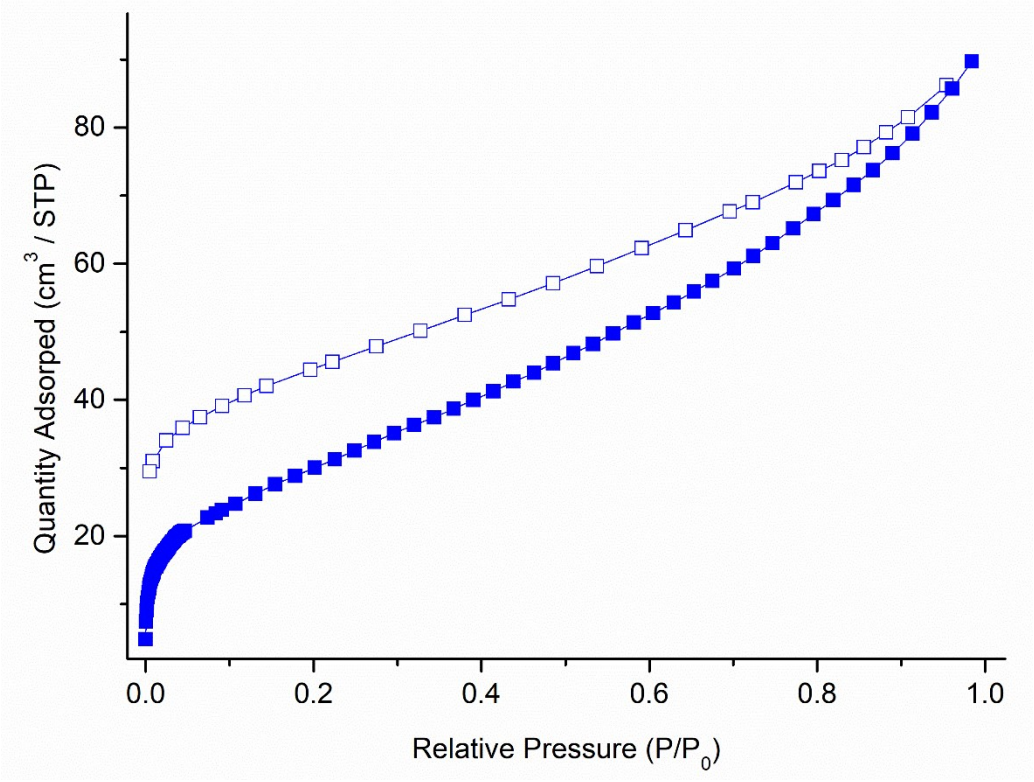

Figure S27. 77k N_2 isotherm of **1**.

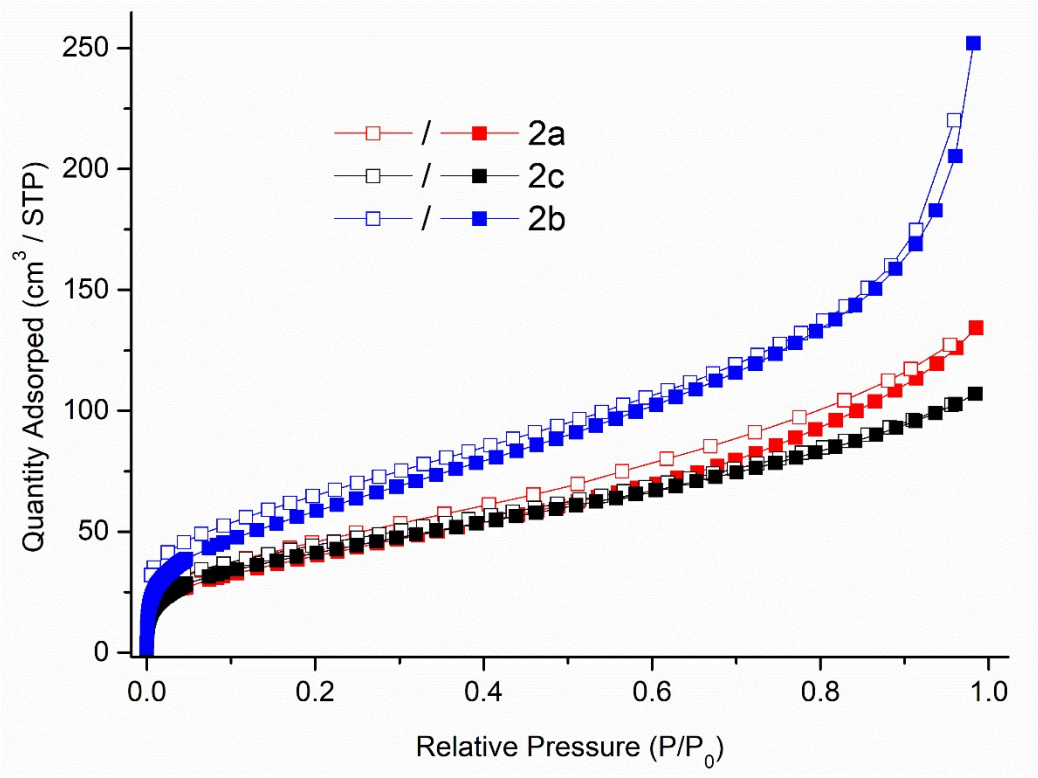

Figure S28. 77k N_2 adsorption isotherm of **2a**, **2b & 2c**.

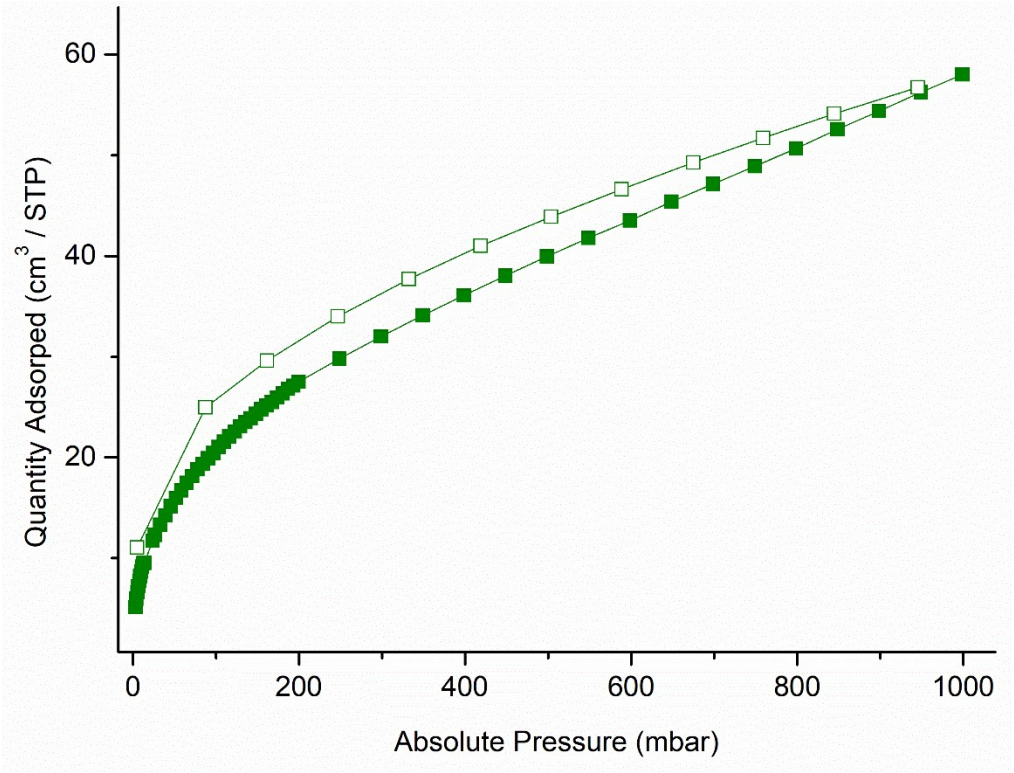

Figure S29. 195k CO_2 isotherm of **1**.

Table S2: BET surface area of **1**, **2a, 2b, 2c**, C^{Boc} & C^{Fmoc} derived from the 77k N_2 isotherm.

Sample	SA_{BET} (m^2/g)
1	62 ± 1.4
C^{Fmoc}	9 ± 0.08
2a	81 ± 1.3
2c	77 ± 0.7
2b	84 ± 2.3

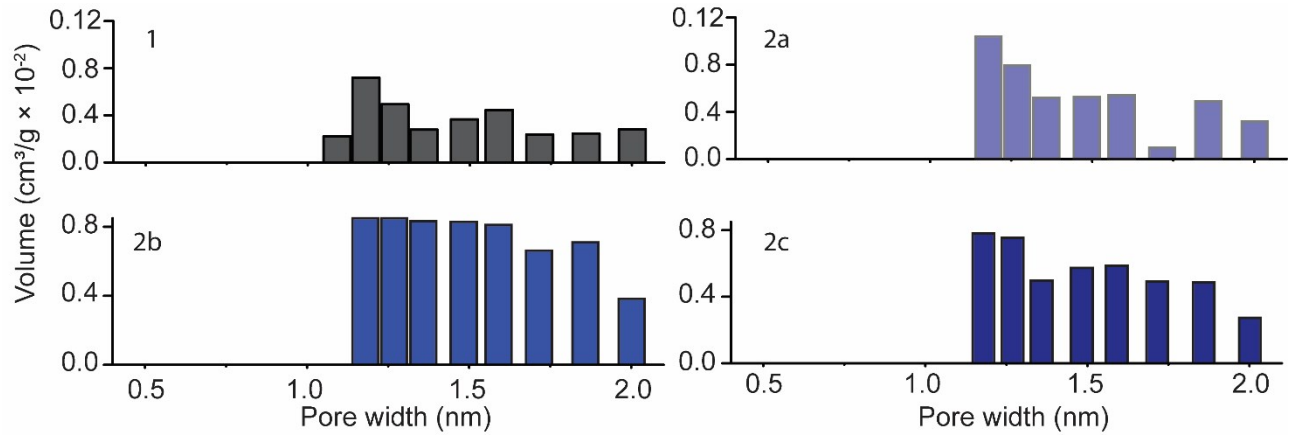

Figure S30. Pore-size distributions (obtained from the low-pressure region of 77 K N_2 isotherms) of **1**, **2a**, **2b**, **2c**.

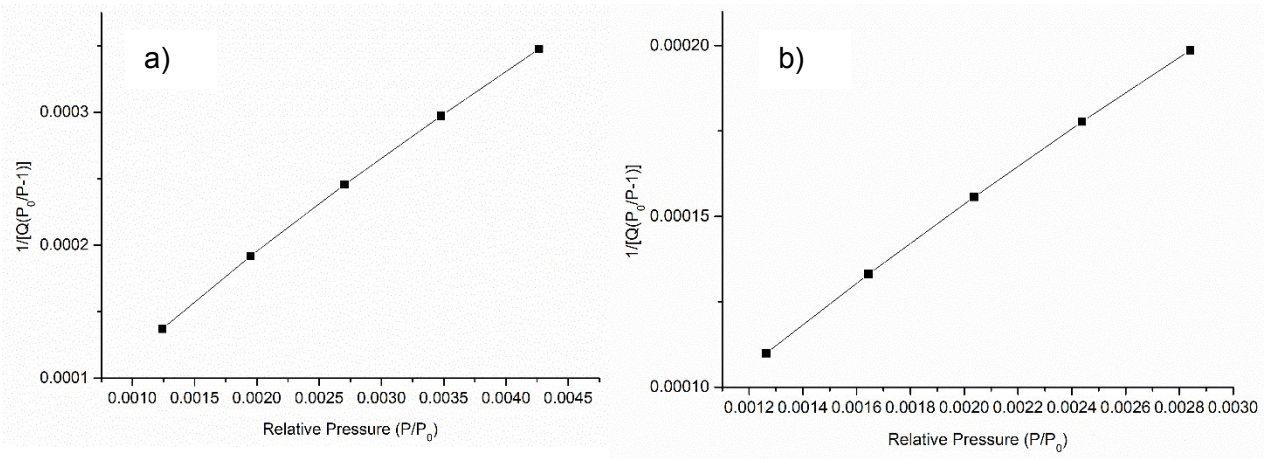

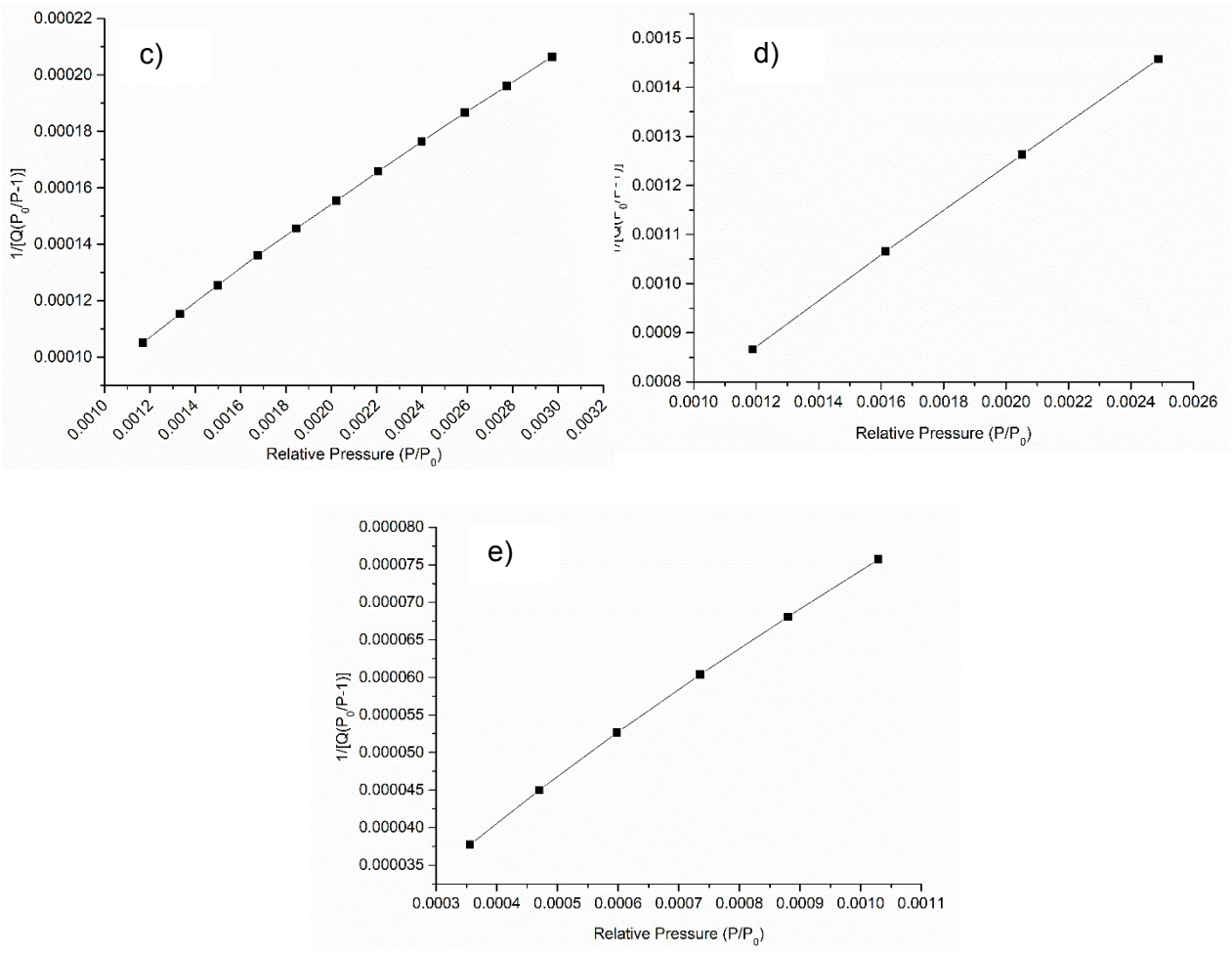

Figure S31. Derivation of the BET surface area from the 77 K N_2 adsorption isotherms for a) **1**; b) **2a**; c) **2c**, d) $\mathbf{C^{Fmoc}}$ & e) **2b**.

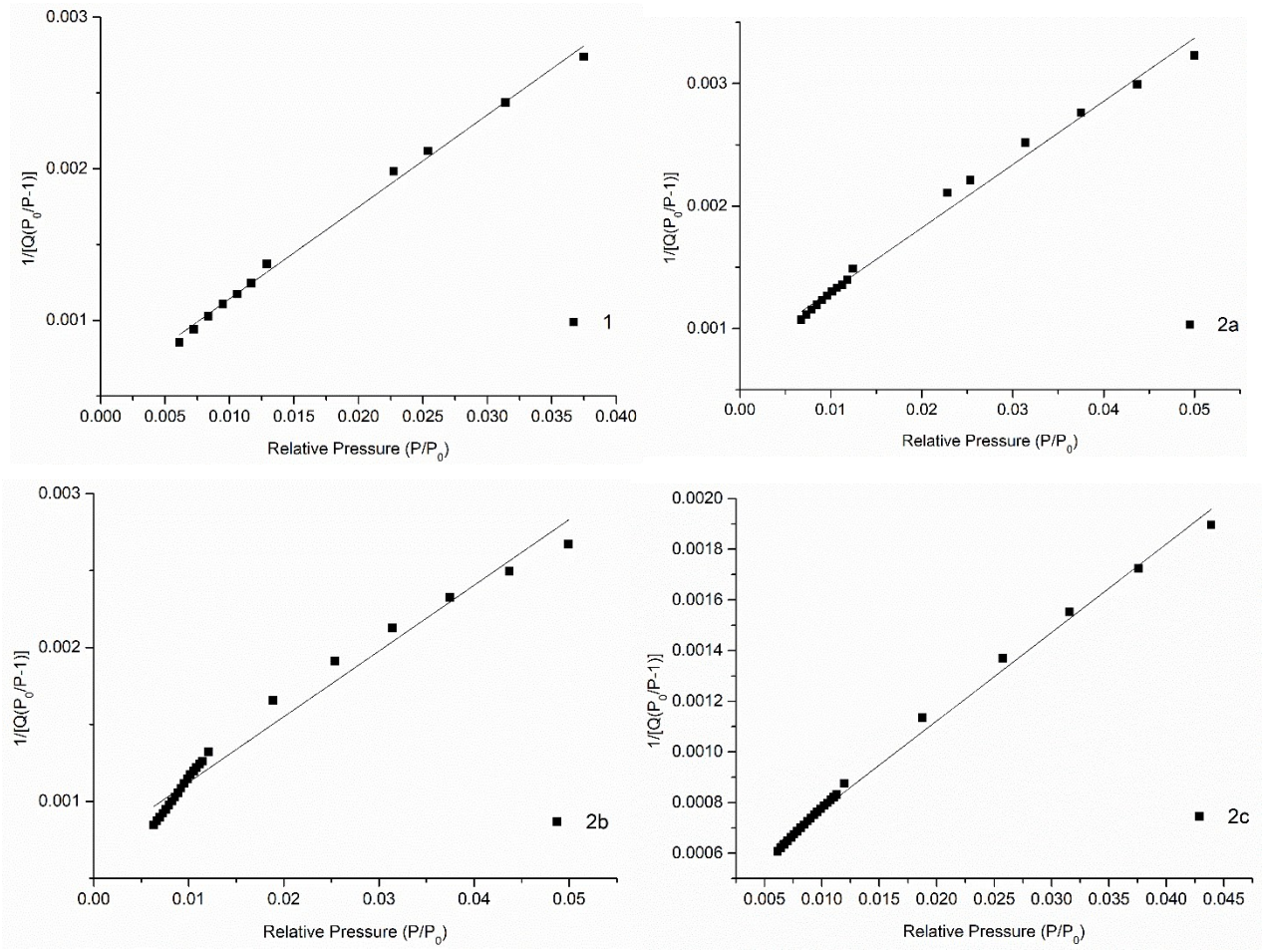

Figure S32. Derivation of the BET surface area from the 195K CO_2 adsorption isotherms for **1**, **2a**, **2b** and **2c**.

Table S3: BET surface area of **1**, **2a, 2b** and **2c**, derived from the 195k CO_2 isotherm.

Sample	SA_{BET} (m^2/g)
1	62 ± 1.3
2a	72 ± 1.8
2b	88 ± 2.9
2c	107 ± 1.5

6. SEM and EDX data of 1, 2a, 2b & 2c.

Scanning Electron Microscope (SEM) images were collected on a Phillips XL30/Quanta 450 scanning electron microscope in secondary electron mode, (spot size 3 and 10 KeV). Electron Dispersive X-ray Analysis was collected with an Oxford Instruments Ultim Max 170 EDX attachment on the Phillips XL30/Quanta 450 (spot size 4, 15 KeV). Samples for SEM analysis were dry loaded onto adhesive carbon tabs on aluminium stubs and carbon coated (5 nm) prior to analysis.

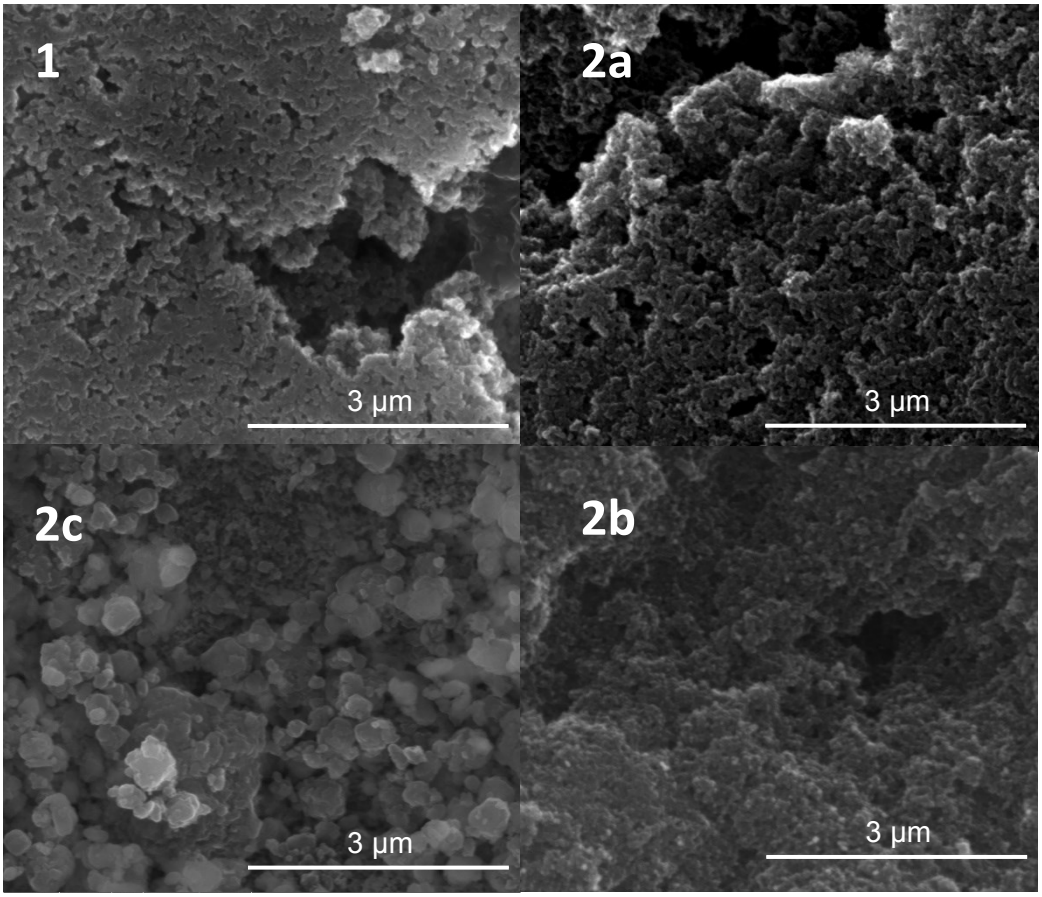

Figure S33. SEM images of **1, 2a**, **2c** & **2b**.

The precipitates were compared via SEM/EDX for morphological and compositional analysis. The Fmoc precipitate was comprised of monodispersed (< 50 nm) spherical particles that pack with no observable ordering. The precipitate **1** was made up of larger monodispersed particles ≈ 50 nm that have more defined edges; however, these particles still appear to be morphologically similar to the Fmoc precipitates (**2a**, **2b**, **2c**) (roughly spherical), and they pack more regularly. EDX analysis of all samples revealed the presence of copper co-localised with carbon, nitrogen and oxygen indicating that the precipitates analysed contained copper species. No standards were utilised, and hence quantitative analysis of copper content is not possible.

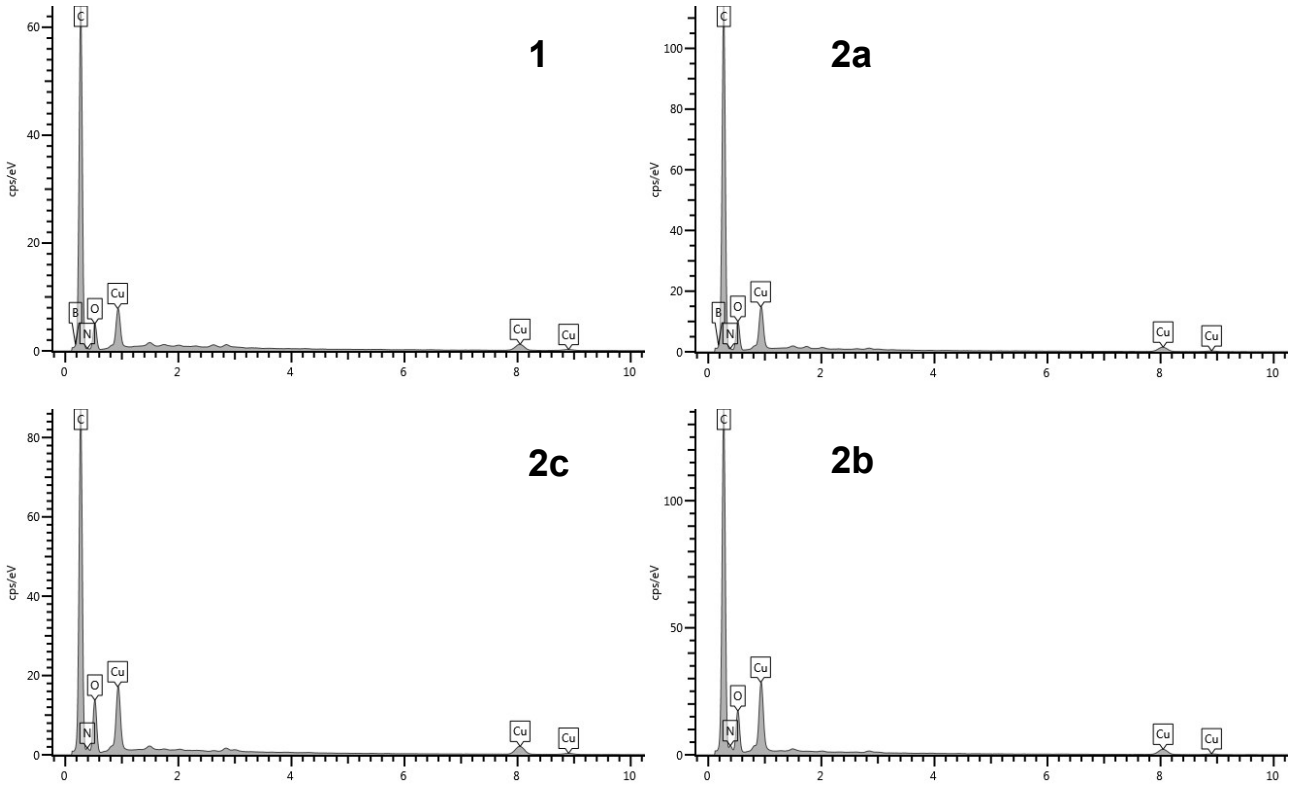

Figure S34. EDX graphs confirming the presence of copper in all of the SCP samples.

7. X-ray crystallography

7.1. General methods

Single crystals were mounted in paratone-N oil on a plastic loop. X-ray diffraction data for $\mathbf{C^{Boc}}$ and $\mathbf{C^{Fmoc}}$ was collected at 100(2) K on the MX-1 beamline of the Australian Synchrotron (λ = 0.7107 Å).[6] Data sets were corrected for absorption using a multi-scan method, and structures were solved by direct methods using SHELXT[7] and refined with SHELXL[8] and ShelXle[9] as a graphical user interface. All non-hydrogen atoms were refined anisotropically and hydrogen atoms were included as invariants at geometrically estimated positions. The refinement of ADP's for carbon, nitrogen and oxygen atoms was supported by similarity restraints (SIMU).[10] The contribution of the electron density from disordered, pore-bound solvent molecules, which could not be modelled with discrete atomic positions were handled using the SQUEEZE[11] routine in PLATON,[12] which strongly improved all figures of merit (FOM). X-ray experimental data is given in Table S3.

Table S3: X-ray experimental data for $\mathbf{C^{Boc}}$ and $\mathbf{C^{Fmoc}}$.

Compound	$\mathbf{C^{Boc}}$	$\mathbf{C^{Fmoc}}$
CCDC number	2013270	2013271
Empirical formula	$C_{120}H_{100}Cu_4N_8O$	C_{168} H_{124} Cu4 N_{12} O_{28}
Formula weight	2356.23	3012.94
Crystal system	Triclinic	Triclinic
Space group	*P*-1	*P*-1
a (Å)	19.294(4)	16.005(3)
b (Å)	19.413(4)	17.777(4)
c (Å)	23.421(5)	20.441(4)
α (º)	72.20(3)	104.91(3)
β (º)	86.15(3)	109.45(3)
γ (º)	65.93(3)	104.86(3)
Volume ($Å^3$)	7609(3)	4912(2)
Z	2	1
Density (calc.) (Mg/m^3)	1.028	1.019
Absorption coefficient (mm^{-1})	0.611	0.486
F(000)	2432	1556
Crystal size (mm^3)	0.15x0.09x0.05	0.05x0.03x0.02
θ range for data collection (º)	0.915 to 23.816	1.140 to 26.371
Reflections collected	42606	61323
Observed reflections [R(int)]	21524 [0.0413]	17261 [0.0184]
Goodness-of-fit on F^2	1.067	1.072
R_1 [I>2σ(I)]	0.0608	0.0655
wR_2 (all data)	0.1888	0.2090
Largest diff. peak and hole (e.Å-3)	0.897 and -0.531	0.941 and -0.757
Data / restraints / parameters	21524 / 1008 / 1456	17261 /719 /959

7.2. Thermal ellipsoid plots

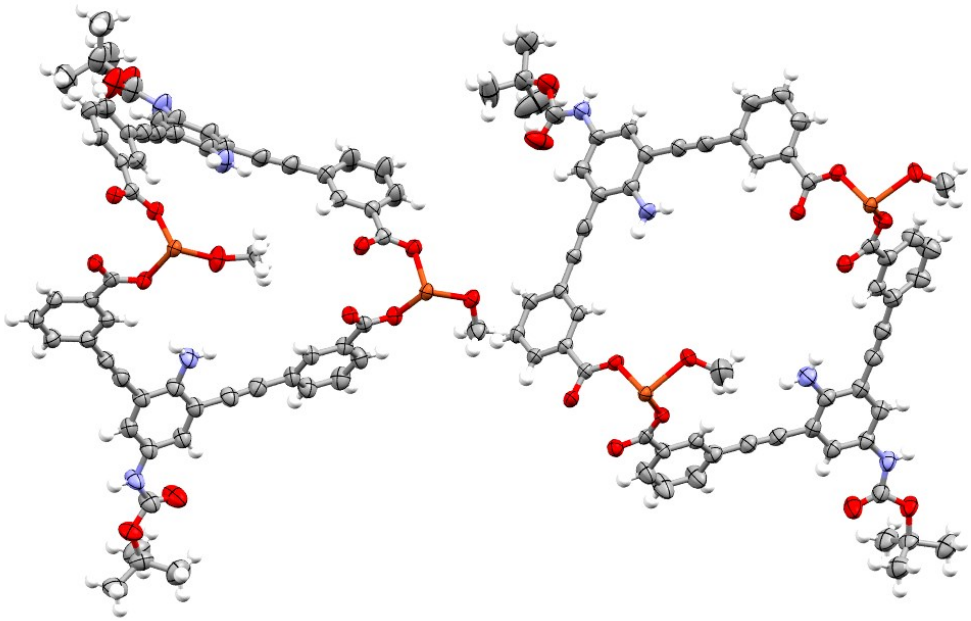

Figure S35. The asymmetric unit of $\mathbf{C^{Boc}}$ with all non-hydrogen atoms shown as ellipsoids at the 50% probability level.

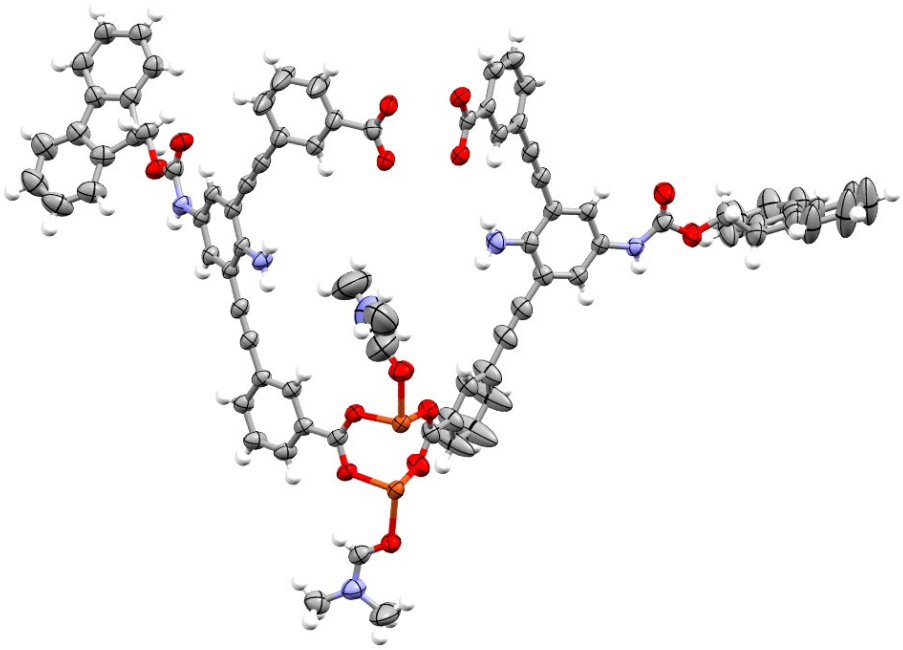

Figure S36. The asymmetric unit of $\mathbf{C^{Fmoc}}$ with all non-hydrogen atoms shown as ellipsoids at the 50% probability level.

8. Cage connectivity in SCPs 2a-c

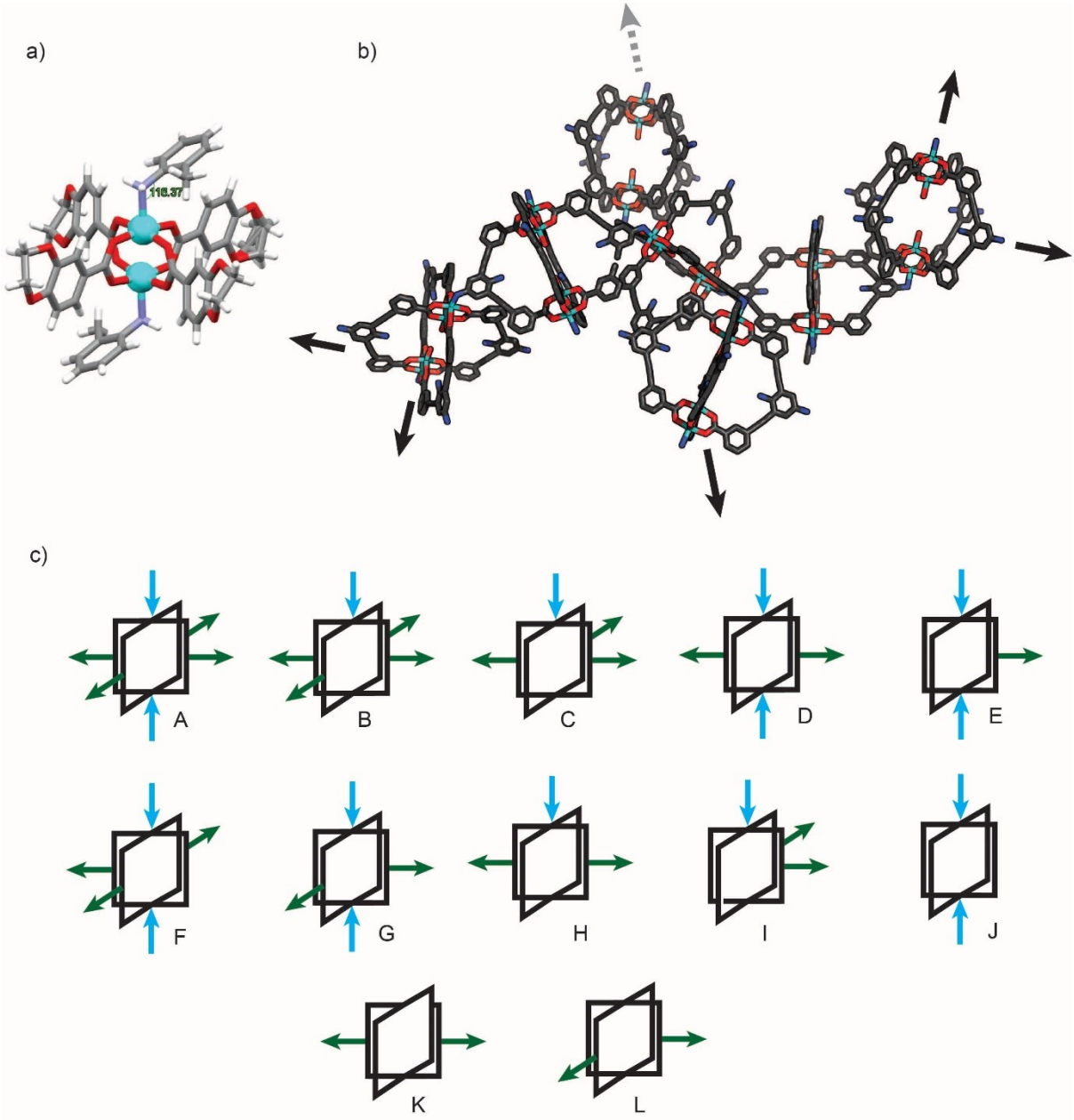

Figure S37. a) X-ray crystal structure of [Cu_2(1,4-benzodioxane-6-carboxylate)$_4$(2-toluidine)$_2$], showing the coordination of 2-toluidine to the axial sites of the Cu_2 paddlewheel (N-Cu – 2.23 Å, C-N-Cu = 116.37°).[13] A SPARTAN model of **2a-c**, based on the above bond distance and angle. The model illustrates that the structure can be feasibly extended in three dimensions; c) possible modes of coordination for the lantern cage (green arrow indicates coordination to the exterior Cu_2 paddle sites, blue arrows indicates coordination from the exterior amine of the phenylenediamine core). As illustrated in the figure, 12 modes of coordination are possible. However, due to the expected steric hindrance, modes A and B are not feasible and the bulk of the structure is likely to be a mixture of motifs C – L.

9. References

1 T. Suzuki, Y. Ota, M. Ri, M. Bando, A. Gotoh, Y. Itoh, H. Tsumoto, P. R. Tatum, T. Mizukami, H. Nakagawa, S. Iida, R. Ueda, K. Shirahige and N. Miyata, *J. Med. Chem.*, 2012, **55**, 9562–9575.

2 V. Brega, M. Zeller, Y. He, H. Peter Lu and J. K. Klosterman, *Chem. Commun.*, 2015, **51**, 5077–5080.

3 W. M. Bloch, R. Babarao and M. L. Schneider, *Chem. Sci.*, 2020, **11**, 3664–3671.

4 V. Brega, M. Zeller, Y. He, H. Peter Lu and J. K. Klosterman, *Chem. Commun.*, 2015, **51**, 5077–5080.

5 S. E. Allen, R. R. Walvoord, R. Padilla-Salinas and M. C. Kozlowski, *Chem. Rev.*, 2013, **113**, 6234–6458.

6 N. P. Cowieson, D. Aragao, M. Clift, D. J. Ericsson, C. Gee, S. J. Harrop, N. Mudie, S. Panjikar, J. R. Price, A. Riboldi-Tunnicliffe, R. Williamson and T. Caradoc-Davies, *J. Synchrotron Radiat.*, 2015, **22**, 187–190.

7 G. M. Sheldrick, *Acta Crystallogr. Sect. A*, 2015, **71**, 3–8.

8 G. M. Sheldrick, *Acta Crystallogr. Sect. C*, 2015, **71**, 3–8.

9 C. B. Hubschle, G. M. Sheldrick and B. Dittrich, *J. Appl. Crystallogr.*, 2011, **44**, 1281–1284.

10 A. Thorn, B. Dittrich and G. M. Sheldrick, *Acta Crystallogr. Sect. A*, 2012, **68**, 448–451.

11 A. Spek, *Acta Crystallogr. Sect. C*, 2015, **71**, 9–18.

12 A. Spek, *Acta Crystallogr. Sect. D*, 2009, **65**, 148–155.

13 G.-H. Sheng, Q.-C. Zhou, J. Sun, X.-S. Cheng, S.-S. Qian, C.-Y. Zhang, Z.-L. You and H.-L. Zhu, *J. Coord. Chem.*, 2014, **67**, 1265–1278.